



Contents lists available at ScienceDirect

Quaternary International

journal homepage: www.elsevier.com/locate/quaint

A late Quaternary record of monsoon variability in the northwest Kimberley, Australia

Emily Field ^{a,*}, Hamish A. McGowan ^a, Patrick T. Moss ^a, Samuel K. Marx ^b

^a School of Earth and Environmental Sciences, The University of Queensland, Brisbane, QLD 4072, Australia

^b GeoQuEST Research Centre, School of Earth and Environmental Sciences, The University of Wollongong, Wollongong, NSW 2522, Australia

ARTICLE INFO

Article history:

Received 28 April 2016

Received in revised form

12 January 2017

Accepted 16 February 2017

Available online xxx

Keywords:

Monsoon
Mound spring
Pollen
Charcoal
Humification
Australia

ABSTRACT

Understanding of the late Quaternary environment of Australia's vast Kimberley region has to date been hindered by the region's lack of classic palaeoenvironmental archives such as deep lake sediments. However, mound spring peat deposits in the region have been found to be a potentially rich archive of palaeoenvironmental data. Here we present a high resolution record from Black Springs mound spring in the Kimberley's northwest, filling some of the current gaps in knowledge of the region's environmental history. This builds on a ~6000 year record developed from the same site and indicates that since the Last Glacial-Interglacial Transition the Australian summer monsoon has varied greatly in intensity, with an increase in monsoonal precipitation from ~14,000 yr BP and pronounced drying in the late Holocene. Despite some chronological uncertainties thought to be due to the inclusion of younger, microscopic root fragments, changes in the record compare well with other records of climatic change from the Kimberley, and across tropical northern Australia.

© 2017 Elsevier Ltd and INQUA. All rights reserved.

1. Introduction

The climate of Australia's vast Kimberley region is dominated by the Australian summer monsoon, which forms part of a wider climate system, including the Indo-Pacific Warm Pool (IPWP) which plays a major role as a global heat source driving planetary scale circulation (Keenan et al., 1989, 2000). Despite a mean annual rainfall of ~1000 mm/yr, high seasonality (>70% of rainfall occurs between January and March) combined with mean annual potential evapotranspiration of ~1900 mm/yr has created a water-limited environment (Bureau of Meteorology (2016)). Consequently, there are few sites that preserve high resolution, unaltered records of palaeoenvironmental change. Many of the lakes and wetlands in the region are seasonally ephemeral, implying that their records may be compromised by desiccation (e.g. leading to aeolian deflation) during the dry season, and by scouring from heavy monsoonal rains and flooding in the wet season (Head and Fullager, 1992). The majority of the high resolution palaeoclimate records that do exist from the Kimberley are from caves (e.g. Denniston et al., 2013a, 2013b, 2015) with only a handful of records of corresponding

vegetation change (e.g. McConnell and O'Connor, 1997; Wallis, 2001; McGowan et al., 2012; Proske et al., 2014; Proske, 2016). As a result the late Quaternary environment and climate of the region and Australia's tropical savannah as a whole remains poorly understood (Reeves et al., 2013).

The Kimberley has a long history of human habitation stretching back ~49,000–44,000 years (Balme, 2000; Fifield et al., 2001; Hiscock et al., 2016). Consequently its archaeological history is of great significance, particularly as it contains one of the greatest concentrations of rock art globally (Aubert, 2012). Understanding the late Quaternary climate of the Kimberley is therefore essential for providing context for this unique archaeological record. The late Quaternary is also a period of significant climatic and environmental change associated with the Last Glacial-Interglacial Transition (LGIT). In this study a ~15,000 year record combining pollen, charcoal, degree of humification and loss-on-ignition (LOI) data is developed from an organic mound spring, Black Springs in the Kimberley's northwest. This record extends and builds on an existing ~6000 year palaeoenvironmental record from the same site (McGowan et al., 2012). The record presented here documents the first humification and LOI data for Black Springs, and the first humification dataset for the Kimberley. Recently acquired surface pollen samples have also been utilised in this study to assist interpretation of the extended pollen record. This study confirms

* Corresponding author.

E-mail address: e.field@uq.edu.au (E. Field).

that, despite the lack of permanent water sources and sediments with good fossil preservation, mound spring peat deposits in the Kimberley are a potentially rich archive of palaeoenvironmental data.

1.1. Mound springs and climate proxies

Peat deposits have been shown to be excellent natural archives of environmental change (Chambers et al., 2012). Whilst the majority of these are located in the high latitudes or high altitude environments (Gaiser and Ruhland, 2010), peat deposits are found in many climatic zones including drier environments, where they are most typically associated with springs (Boyd and Luly, 2005). An organic mound will only form at a spring where outflow is higher than the rate of evaporation, thereby preventing desiccation and mineralisation and where discharge is sufficiently low to prevent mound erosion (Ponder, 1986). Most commonly mounds are derived from aeolian deposits, precipitated calcium carbonate, or silicates in volcanic provinces (McCarthy et al., 2010). However, mounds comprised of peat will also form where there is sufficient water in otherwise challenging environments (Boyd, 1990a). Examples include those in the Australian arid and tropical zones (e.g. Boyd, 1990b; Boyd and Luly, 2005; McGowan et al., 2012), in the East African arid zone (e.g. Owen et al., 2004) and in South Africa (e.g. Scott, 1982a, 1982b, 1988; Scott and Vogel, 1983; Scott and Nyakale, 2002).

Organic mound springs are classed as minerotrophic since water is derived largely from artesian aquifers as well as meteoric sources (Barber and Charman, 2005; Backwell et al., 2014). These springs develop with distinct stages of growth, outlined by Ponder (1986). A juvenile spring typically forms in a small depression which infills with runoff derived alluvium and aeolian sediments, precipitates from groundwater and decomposing vegetation. In these early stages spring discharge is typically vigorous with a pool forming at the vent and outflow channels conveying the water into a wetland or spring “tail”. The presence of a perennial water source enables the establishment of vegetation at the spring, with subsequent decomposition of this vegetation contributing to mound growth. As time progresses and the peat mound increases in size less alluvial runoff-derived sediment is incorporated into the spring. When a spring is active the buried peats remain relatively fresh due to anaerobic conditions and/or the waterlogged nature of the site (Backwell et al., 2014) with capillary creep and outward diffusion of water through the mound limiting oxidation (McCarthy et al., 2010). Groundwater outflow and peat wetness is related to meteoric recharge via pressure transmitted through the aquifer regardless of water retention time (McCarthy et al., 2010). Humification, a proxy for bog surface wetness, will reflect changes in outflow which in this environment is assumed to reflect long term patterns (hundreds to thousands of years) in precipitation which drives aquifer recharge. Spring development and morphology can be reflected in both the fossil pollen assemblages (Boyd, 1990b) and the changing organic content at the site from which secondary conclusions about climatic conditions can be made given knowledge of modern vegetation distributions in relation to climate (Moss, 2013). Charcoal accumulation can provide insight into local and regional fire activity (Mooney and Tinner, 2011).

This study uses multiple measures of mound spring conditions to produce a robust, high resolution reconstruction of changes in the strength of the Australian summer monsoon since the LGIT, whilst also providing a record of spring development and morphology. This record will provide context for ongoing archaeological research in the Kimberley and increase current understanding of the region's late Quaternary climate.

2. Regional setting

2.1. Location and hydrogeology

Black Springs (15.633°S; 126.389°E) is a peat mound spring located in the North Kimberley Bioregion (Government of Western Australia, 2011) (Fig. 1). The peat mound is fed by freshwater from local aquifers of low to moderate productivity within the Kimberley's fractured rock province, distinct from the highly productive extensive aquifers of the Canning and Bonaparte sedimentary basins to the east and west, respectively (Brodie et al., 1998). The mound stands ~2 m above the surrounding terrain with organic material comprised predominantly from decomposing vegetation that is growing on the mound.

2.2. Climate

Precipitation in the Kimberley is dominated by the Australian summer monsoon and tropical cyclones, both of which typically occur during the austral summer between December and March (DJFM) associated with the seasonal southward migration of the Inter-Tropical Convergence Zone (ITCZ) (Suppiah, 1992). The monsoon trough separates the trade winds to the south and westerlies to the north, with strong convection embedded in the latter (McBride, 1987). Active monsoon periods correspond with a more southerly position of the monsoon trough over the Pilbara Heat Low, whereas weaker monsoon activity corresponds with a more northerly ITCZ position (Suppiah, 1992). Mean annual precipitation (1988–2016) at Drysdale River Station, 7.8 km from Black Springs, is 1110 mm/yr with the vast majority (on average 908 mm) falling during the summer (DJFM). Temperature data from Doongan Station (1988–2016, 29.2 km from Black Springs) indicates that there is little variation in temperature throughout the year (33.2 °C in January and 29.7 °C in July) with an average annual temperature of 33 °C (Bureau of Meteorology (2016)).

A number of modern drivers of climate variability affect the strength of the Australian summer monsoon. The 40–60 day Madden-Julian Oscillation (MJO) alters the strength of westerly airflow into the monsoon trough (Wheeler et al., 2009), and the IPWP to the north of the Kimberley acts as a key source of moisture and heat to the atmosphere (Huang and Mehta, 2004) fuelling monsoon activity across tropical Australasia. Variability in sea surface temperatures (SSTs) is also a key factor driving Australian rainfall patterns (Taschetto et al., 2010). The El Niño/Southern Oscillation (ENSO) operates over a 3–7 year cycle and is the most influential driver of Australian rainfall variability in the tropical north during the austral summer (Risbey et al., 2009). ENSO is embedded within the Walker Circulation, which under normal conditions is associated with convection over Indonesia and subsidence over the eastern Pacific (McPhaden, 2004). During El Niño events the location of subsidence is near Australia which can disrupt moisture advection and suppress rainfall over the region (Jourdain et al., 2013). In northwest Australia (including the Kimberley) the impacts of ENSO are currently subdued (McBride and Nicholls, 1983; Bureau of Meteorology (2016)), but may have been more significant in the past. Despite the current muted influence of ENSO, La Niña events (which result in increased spring and summer precipitation in the Kimberley) and strong El Niño events, such as in 1982–1983 (which resulted in decreased precipitation), can cause significant rainfall variability over northwest Australia (Bureau of Meteorology (2016)). Similarly, during El Niño Modoki events, which are characterised by warm SSTs in the central Pacific Ocean and anomalously cool SSTs in the west and east (i.e. a double Walker circulation) (Ashok et al., 2007), the monsoon in northwest Australia is shorter yet more intense due to the anomalous cyclonic

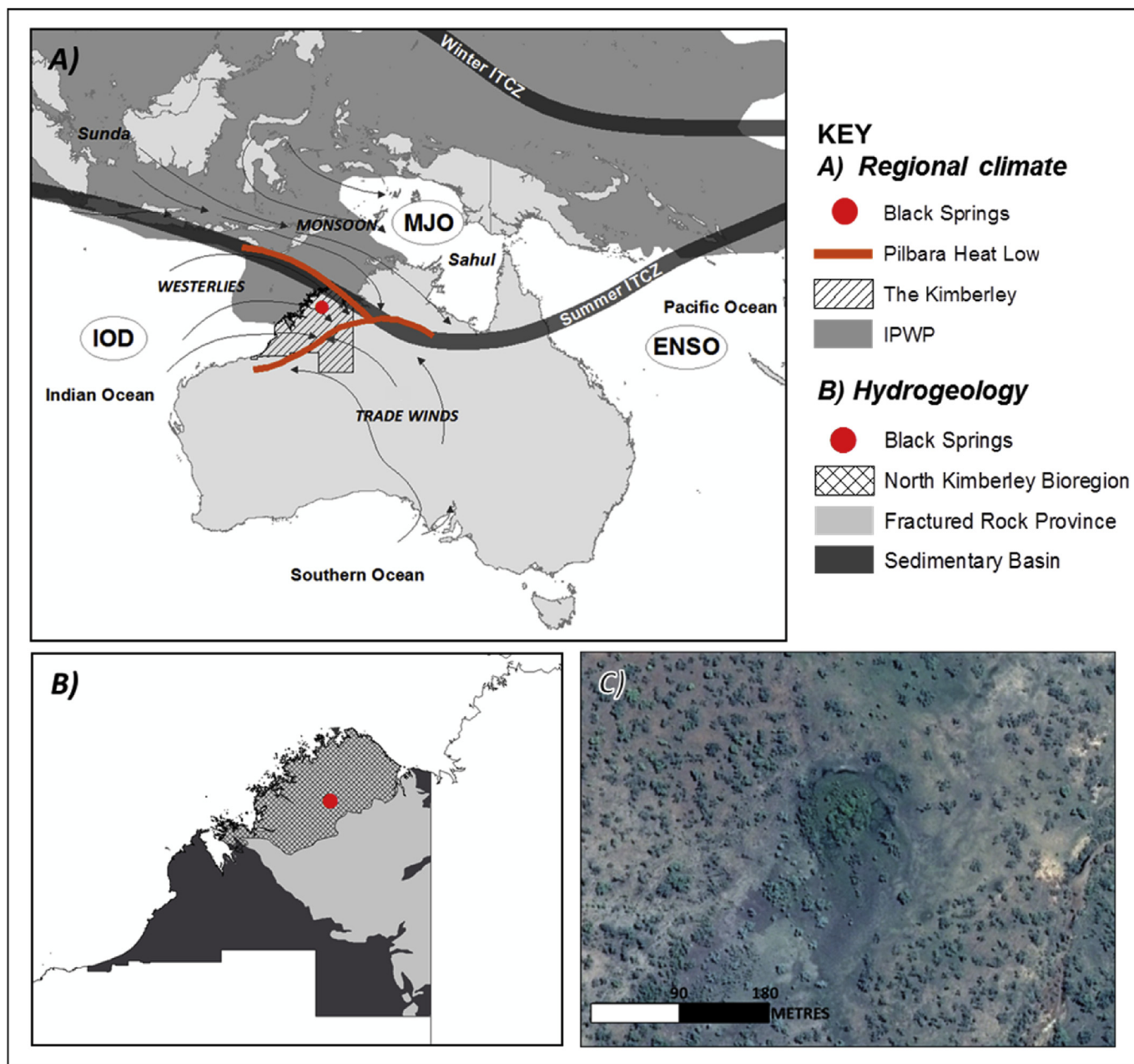


Fig. 1. Location of Black Springs in relation to (A) Australian climatic features (IPWP adapted from Gagan et al. (2004) and Pilbara heat low and wind patterns adapted from Kuhnt et al. (2015)), (B) regional hydrogeologic units of the North Kimberley Bioregion, and (C) satellite imagery of the Black Springs study site - the mound is visible as the dark green patch in the centre of the image (Google Earth imagery captured 22.11.2015). (For interpretation of the references to colour in this figure legend, the reader is referred to the web version of this article.)

circulation which strengthens warm moist westerly airflow into the monsoon trough (Taschetto et al., 2010).

Over longer timescales there is evidence of change in the frequency and intensity of ENSO. Both climate models and palaeorecords indicate that the frequency and/or amplitude of ENSO may have increased from the mid Holocene (e.g. Shulmeister and Lees, 1995; Moy et al., 2002; Gagan et al., 2004; Conroy et al., 2008; Marx et al., 2009), with a particularly sharp intensification from ~3700 yr BP until at least 2000 yr BP (Donders et al., 2007), before a decline for the period 1500–1000 yr BP (Rein et al., 2004; Stott et al., 2004). There is inconsistency between records, however, with some corals from the Pacific contradicting the inferred Holocene changes in ENSO previously described (McGregor and Gagan,

2004; Cobb et al., 2013). Given the current muted effects of most ENSO events in the Kimberley, it is unclear as to what extent past changes in ENSO would have impacted northwest Australia. However, it is worth noting that the relationship between ENSO and precipitation can change through time (e.g. Webster and Palmer, 1997). For instance, the intensity of ENSO phases (El Niño and La Niña) is modulated by the Inter-decadal Pacific Oscillation (IPO) whereby El Niño (La Niña) is suppressed (enhanced) during its positive (negative) phase (Power et al., 1999). In a similar manner the Indian Ocean Dipole (IOD) can influence the effects of ENSO phases on the climate of northern Australia, with concurrent El Niño and positive IOD events leading to an increased probability of below average rainfall (Meyers et al., 2007). Changes in frequency

and intensity of both ENSO phases in response to, for example, longer multi-decadal variability in the IPO and interactions with other teleconnections such as the IOD therefore modulate the Australian monsoon. Mechanisms such as these have been proposed for “entrenched” El Niño or La Niña states argued to be driving changes in records obtained by Koutavas et al. (2002) and Stott et al. (2002). Thus ENSO may have impacted this study region more significantly in the past. Denniston et al. (2013b; 2015) suggest that a change in mean state could have created a stronger coherency between ENSO and the monsoon in Australia's north-west since the mid Holocene albeit with this connection weakening at some stage in the last millennium, whilst the results of complex network analysis by McRobie et al. (2015) also raise the possibility of an ENSO teleconnection to northwest Australia in the late Holocene (from 3000 yr BP).

2.3. Regional and mound spring vegetation

The Kimberley's vegetation is predominantly tropical savanna, punctuated by shrublands, bunch grasslands, sedgeland, herblands, rainforest, and desert dunes (Government of Western Australia, 2011; Department of Environment and Conservation (2012)). Black Springs is located within an area of tropical savanna comprised of grass, trees and shrubs (Department of Environment and Conservation (2012)), including *Grevillea* and abundant *Eucalyptus* and *Acacia* (Fig. 2). The vegetation upon the mound itself is distinct from the surrounding savanna with a dense forest of wetland and monsoon vine thicket including *Melaleuca viridiflora*, *Ficus*, *Timonius timon* and *Pandanus spiralis*. Vegetation in the fringing spring-fed wetland is dominated by sedges and perennial *Phragmites karka* grassland (Department of Environment and Conservation (2012) and field observation).

3. Materials and methods

3.1. Sample collection

A 1.68 m peat core was collected from Black Springs during the dry season in July 2005. The core was sub-sampled with an average sample width of 7 mm. To assess pollen assemblages in various spring micro-habitats and to aid palaeoenvironmental interpretation, five surface samples were collected during the dry season in June 2015. Surface “grab” samples of ~10 g wet weight were taken along a ~150 m transect extending from the highest point of the mound into the surrounding tropical savannah (Fig. 4).

3.2. Chronology

Eleven samples (initially nine pollen concentrate samples followed by two bulk samples in an effort to understand age reversals in the pollen concentrate dates) through the core were dated by accelerator mass spectrometry (AMS) radiocarbon (^{14}C) dating. Pollen concentrate was separated for dating following Moss (2013). Samples were submitted to the Waikato Radiocarbon Dating Laboratory where they were pre-treated using the AAA method before being graphitised and prepared for AMS ^{14}C measurement. Conventional ^{14}C ages were calibrated to calendar years before present (cal. yr BP) using OxCal V4.2.4. (Bronk Ramsey, 2013) and SHCal13 (Hogg et al., 2013) with 0 cal yr BP representing 1950 A.D. A Bayesian age-depth model was constructed for the core using Bacon 2.2 (Blaauw and Christen, 2011).

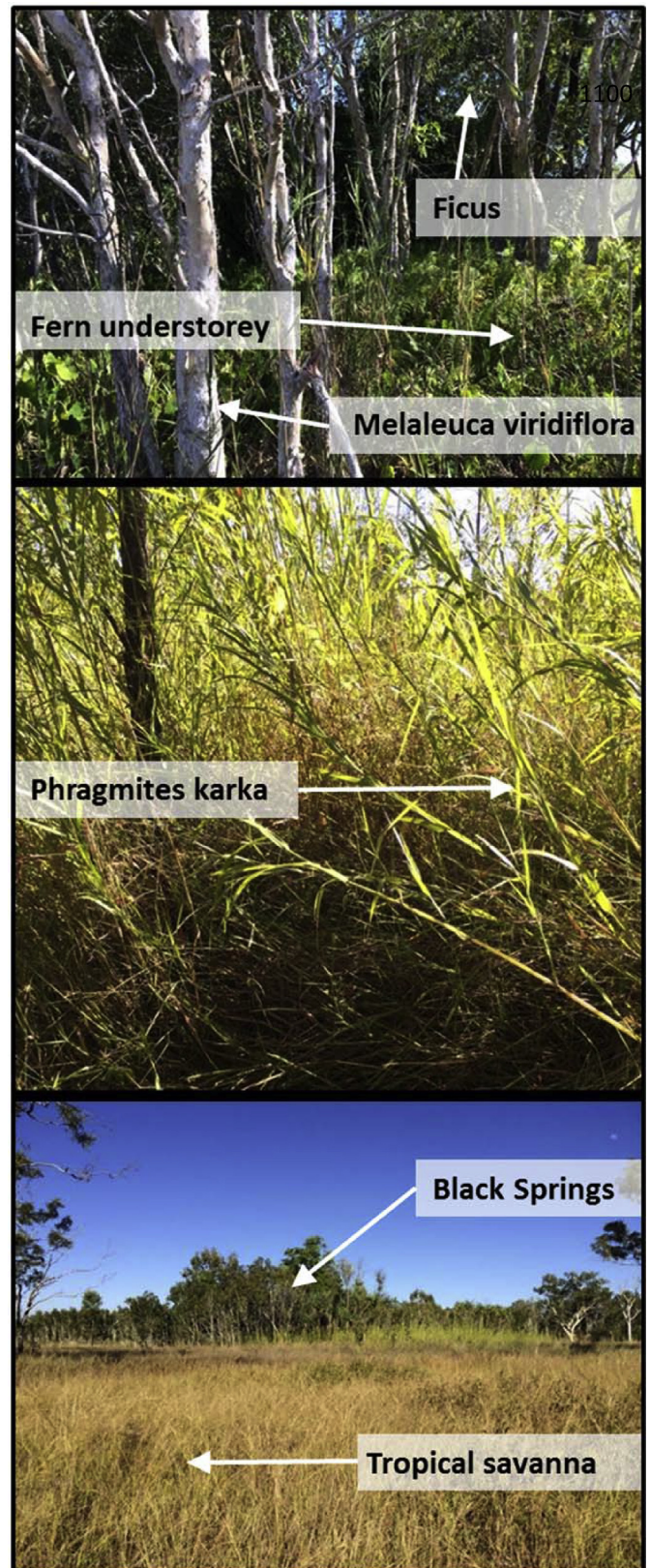


Fig. 2. Photographs of Black Springs. The top plate shows mound spring vegetation including *Ficus*, *Melaleuca viridiflora* and a fern understorey; the centre plate shows the fringing *Phragmites karka*; the bottom plate shows surrounding tropical savanna grassland.

3.3. Pollen and microcharcoal analysis

Pollen analysis was undertaken on 105 down-core samples and 5 surface samples. With the exception of one down-core sample at 20.5 cm all contained pollen. Core samples consisted of 2 cm³ of dried material, while surface samples consisted of 1 cm³ of wet material.

Pollen and micro-charcoal analysis followed Moss (2013), whereby samples were disaggregated using 10% tetrasodium pyrophosphate (Na₄P₂O₇) heated to 100 °C. Disaggregated samples were passed through 180 µm and 8 µm sieves, with the >8 µm retained fraction being treated with 8% potassium hydroxide (KOH) to remove humic acids. Sodium polytungstate (Na₆(H₂W₁₂O₄₀)) at a specific gravity of 1.9 was used to separate remaining minerogenic material from the pollen using centrifugation. The remaining organic fraction underwent acetolysis to dissolve excess organic material and stain palynomorphs for easier identification using a 9:1 ratio of acetic anhydride ((CH₃CO)₂O) and concentrated sulfuric acid (H₂SO₄) heated to 90 °C. *Lycopodium clavatum* (an exotic marker spike) was added to each sample to enable calculation of pollen, charcoal and non-pollen palynomorph concentrations (expressed per cm³). Pollen, charcoal and non-pollen palynomorph accumulation rates (expressed per cm³ per year) were calculated using these concentrations and the growth rates presented in Section 4.1. Pollen/micro-charcoal samples were mounted in glycerol (C₃H₈O₃) on slides and counted using light microscopy at 400× magnification, with palynomorph identification utilising the Australasian Pollen and Spore Atlas (APSA Members, 2007). The pollen sum consisted of 200 pollen grains (excluding aquatic taxa and pteridophyte spores), or two completely counted slides. If the 200 grains were encountered in under ten transects, a total of ten transects were counted to capture a good representation of the slide. Counts are expressed as a percentage of the total pollen sum. The charcoal sum used to calculate charcoal concentrations consisted of all black angular pieces of >5 µm counted across three evenly spaced transects.

Fossil pollen data was collated and plotted using Tilia (Grimm, 1991) and TGView software (Grimm, 2004) with identification of zones guided using CONISS (Grimm, 1987). Multivariate statistics were used to identify floristic patterns in both the fossil and modern pollen datasets, and to compare fossil and modern assemblages. Ordinations were performed using CANOCO 4.54 (Ter Braak and Šmilauer, 2002) and plotted using CanoDraw 4.13 (Ter Braak and Šmilauer, 2002) and included the pollen, spore and non-pollen palynomorph data. Two samples (at 39 cm and 95.5 cm)

were statistical outliers and were excluded from these analyses. Detrended Correspondence Analysis (DCA) with detrending by segments was used to determine whether linear or unimodal analysis was appropriate based on the length of the first axis, and the data subsequently examined using the linear technique Principal Components Analysis (PCA) following Ter Braak and Prentice (1988).

3.4. Sediment analysis

Loss-on-ignition (LOI) analysis was performed on 230 contiguous samples with the exception of 2 samples (at 113 cm and 164 cm) where no sample remained following ¹⁴C analysis. Samples were dried at 105 °C and weighed, then placed in weighed and pre-baked crucibles and combusted at 500 °C, before finally being weighed at room temperature. Weights were then used to calculate the percentage of organic material in each sample following Heiri et al. (2001).

3.5. Humification analysis

Peat humification followed the standard alkali-extraction method of Chambers et al. (2011). Measurements were made on 114 alternate samples, with samples consisting of 0.2 g ground and dried material (60 °C). Humic materials were disaggregated from samples through treatment with 8% sodium hydroxide (NaOH) heated at 95 °C. Samples were passed through 11 µm filter paper and diluted to 25%. An aliquot of each sample was measured for % light transmission and absorbance (3 repeats) in 1 cm diameter polystyrene cuvettes on a GBC Cintra UV–vis spectrophotometer stabilised at 540 nm with de-ionised water as zero standard. Percentage transmission values were normalised to LOI following Blackford and Chambers (1993), a step necessary to remove the anomalously high % transmission values produced by the peats of higher mineral content at the base of the core. This is required since it is likely that the deeper LOI values are predominantly related to mound spring morphology and do not wholly reflect changes in spring surface wetness. Following Burrows et al. (2014), the normalised data was smoothed using a three point moving average in order to reduce artefacts produced by aberrant values, and detrended by applying a fourth order polynomial (residual values plotted) to remove the impact of catotelm decay and to emphasise high frequency shifts.

Table 1

Radiocarbon dates and calibrated ages for Core BSP. Radiocarbon dates incorporated in the age model are shown in bold, italicised text.

Lab code	Uncalibrated ¹⁴ C age	Depth (cm)	Calibrated age (cal. yr BP) ^a	Fraction dated
Wk-29127	516 ± 35	22.5	514 ± 8 (100%)	Pollen
Wk-28374	3455 ± 30	45	3655 ± 43 (100%)	Pollen
Wk-29128	4671 ± 32	55	5424 ± 23 (75%)	Pollen
			5319 ± 8 (25%)	
Wk-29129	6938 ± 37	79	7720 ± 44 (89%)	Pollen
			7779 ± 8 (11%)	
Wk-28376	8186 ± 35	94.5	9070 ± 56 (100%)	Pollen
Wk-29130	7081 ± 40	104	7887 ± 51 (100%)	Pollen
Wk-41825	6151 ± 84	112.7	7017 ± 134 (100%)	Bulk peat
Wk-28377	5713 ± 30	126.5	6450 ± 42 (100%)	Pollen
Wk-29131	7439 ± 36	140	8273 ± 31 (58%)	Pollen
			8197 ± 21 (42%)	
Wk-28375	7033 ± 31	152.5	7827 ± 38 (82%)	Pollen
			7912 ± 10 (18%)	
Wk-41826	5437 ± 22	164.3	6254 ± 22 (56%)	Bulk peat
			6204 ± 18 (44%)	

^a OxCal V.4.2.4 (Bronk Ramsey, 2013), 1σ error.

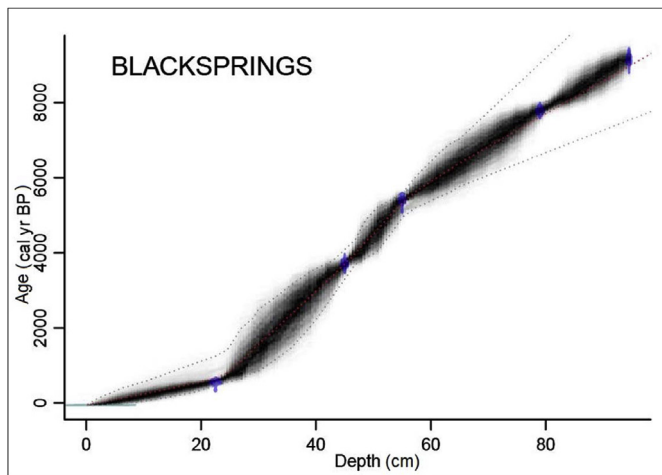


Fig. 3. Bayesian age model generated for the Black Springs core. The age model was generated using Bacon 2.2 (Blaauw and Christen, 2011). The blue dots represent the radiocarbon ages. (For interpretation of the references to colour in this figure legend, the reader is referred to the web version of this article.)

4. Results

4.1. Chronology

^{14}C results are presented in Table 1. The Bayesian age-depth model (Fig. 3) suggests that the core spans the last ~15,000 years and shows clear shifts in growth rates, although these are partly a function of the discrete radiocarbon sampling methodology and Bayesian model applied. Average growth rates (uncorrected for compaction) are 0.11 mm/year from the base of the core until ~5400 cal yr BP, subsequently decrease over much of the late Holocene (0.07 mm/year) until ~500 cal yr BP, following which they increase to 0.44 mm/year.

Dates from the top 94.5 cm of the core returned a coherent age/depth relationship, however age reversals are present throughout the lower section of the core. *Phragmites karka* is found growing abundantly across Black Springs, a species known to transport modern carbon into deep sediments via its extensive root system (Boyd, 1990b). It is therefore likely that young carbon has been incorporated into the lower stratigraphic units via root growth. Strikingly similar issues with ^{14}C dating are evident at other peat mound springs in both Australia (Boyd, 1990b; Macphail et al., 1999) and South Africa (Scott, 1982b; Scott and Vogel, 1983; Van Zinderen Bakker, 1995; Scott et al., 2003; Backwell et al., 2014). Macroscopic analysis by Scott and Vogel (1983) confirmed tiny rootlets were present throughout the sediments from Rietvlei dam, South Africa probably resulting in the age reversals and erroneously young dates encountered. A subsequent effort by Scott and Nyakale (2002) to remove rootlets from ^{14}C sub-samples at Florisbad Spring, South Africa resulted in a tighter chronology suggesting that rootlets are a primary source of dating problems at mound spring sites.

Due to the potentially contaminated deeper ^{14}C ages all dates below 94.5 cm have been excluded from the age model giving a maximum constrained age of 9070 cal yr BP (Fig. 3). If the age model is extrapolated using the growth rate for the lower section of the core, it suggests a basal age of approximately >15,000 cal yr BP at 1.66 m. However, all age estimations below 94.5 cm should be considered with caution given the uncertainties in extrapolation of the age model to deeper sections of the mound. Therefore, this paper treats ages older than 9070 cal yr BP as approximate. It is also possible that root contamination may have affected the sediments

<94.5 cm despite the coherency of the age-depth relationship in this section of the core. Nonetheless, the results presented both here and previously by McGowan et al. (2012) show strong similarities in the timing of environmental change with previously published records for northern Australia giving us confidence in our chronology of climatic and environmental change developed here for the entire core.

In an effort to test the validity of the age model tie points between the Black Springs fossil record and other records from the region were identified. This method is common where ^{14}C chronologies contain uncertainty (e.g. Scott and Vogel, 1983; Macphail et al., 1999; Moss et al., 2013). Peaks in biomass burning (recorded by fossil charcoal) previously identified in the Australian tropics and centred at 8000 cal yr BP and 11,500 cal yr BP, as well as a reduction in biomass burning from ~7500 to 5000 cal yr BP (Mooney et al., 2011), are recorded in the Black Springs charcoal record at these times (see Fig. 7). Similarly, increases in grass during the last millennium in the northern Kimberley (Proske, 2016) and in the Northern Territory (Shulmeister, 1992) are also mirrored in the Black Springs pollen record (see Fig. 5). Coherence in the timing of these changes between the Black Springs and other palaeoenvironmental records imply the Black Springs age model is broadly accurate.

4.2. Surface pollen

Table 2 lists the 33 taxa identified in the surface samples and their ecological affinities, whilst Fig. 4 contains summary pollen plots for each sample and a PCA biplot for the dataset. Pollen assemblages in the five surface samples reflected the current immediate vegetation. Sample MP3-5, collected from the tropical savanna surrounding the spring is, unsurprisingly, dominated by Poaceae (56.3%) and has the highest amount of tropical savanna taxa of all surface samples (19.5%). The PCA confirms tropical savanna taxa are closely associated with this sample including *Eucalyptus* which comprises a majority of the trees in the savanna. Sample MP2-4, collected from the marshy wetland in the spring tail is dominated by wetland taxa (43%) and in particular by the sedge Cyperaceae (33.4% of the total pollen sum). Poaceae pollen is also abundant in this sample (27%), however given that *Phragmites* is thought to contribute little to pollen grass assemblages (e.g. Haslam, 1972; Kershaw, 1979; Hall, 1989, 1990) it is likely that the majority of the Poaceae pollen observed in this sample, and indeed the other modern and fossil pollen samples, is derived from the savanna surrounding Black Springs rather than the *Phragmites* growing in the wetland. The PCA also indicates that Cyperaceae and ferns are closely aligned with this sample. Sample MP0-3, collected from the partially inundated lower slopes of the mound with a water depth of ~5 cm shows a dramatic increase in spring taxa (40%), with the PCA confirming that *Melaleuca* is most closely associated with this sample, probably derived from the abundant *Melaleuca viridiflora* growing on the mound. *Cynogeton dubium*, a perennial aquatic indicative of pools of water, is also most closely associated with this sample which is to be expected given the water depth. Samples D4-2 and MP1-1 located on the peat mound are unsurprisingly dominated by spring taxa (57.3% and 58.2% respectively), in particular MP1-1 which is located in the centre of the mound where the water table is at or near the surface. The PCA reveals that taxa including *T. timon*, *Pandanus*, *Mallotus*, *Euphorbia* and *Ficus* are closely allied with sample MP1-1 reflecting the monsoon vine thicket growing on the mound. The non-pollen palynomorph *Pseudochizaea* is most abundant in sample D4-2 which was the driest sample (water table 19 cm below surface) and located on the shoulder of the mound. *Pseudoschizaea* is thought to be an algal cyst with highest abundances in damp soils

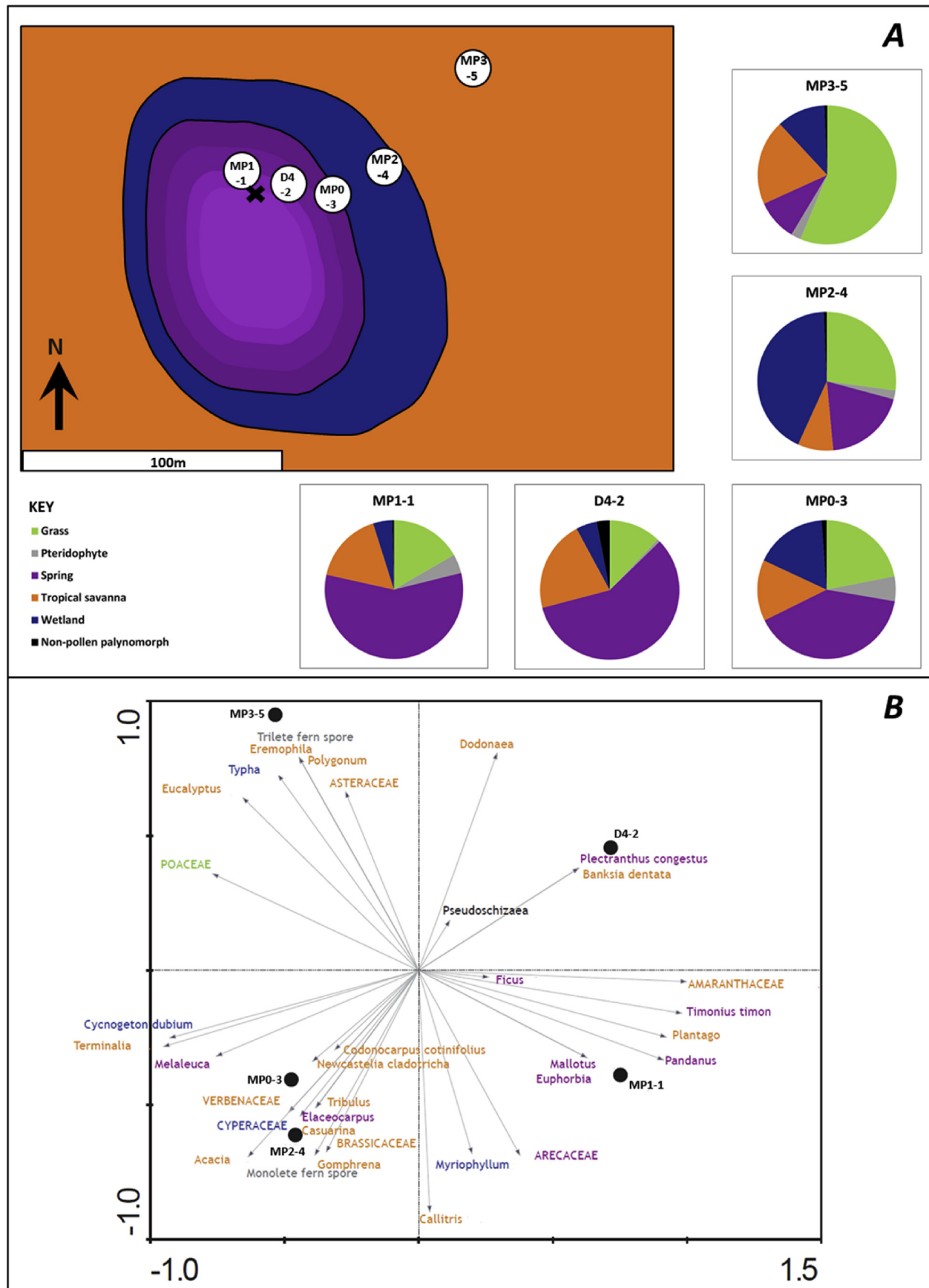


Fig. 4. (A) Map showing the vegetation zones of Black Springs. The position of surface sample locations is indicated on the panel, while the composition of each surface sample is indicated in the pie charts. (B) PCA biplot of the surface samples shown in panel A.

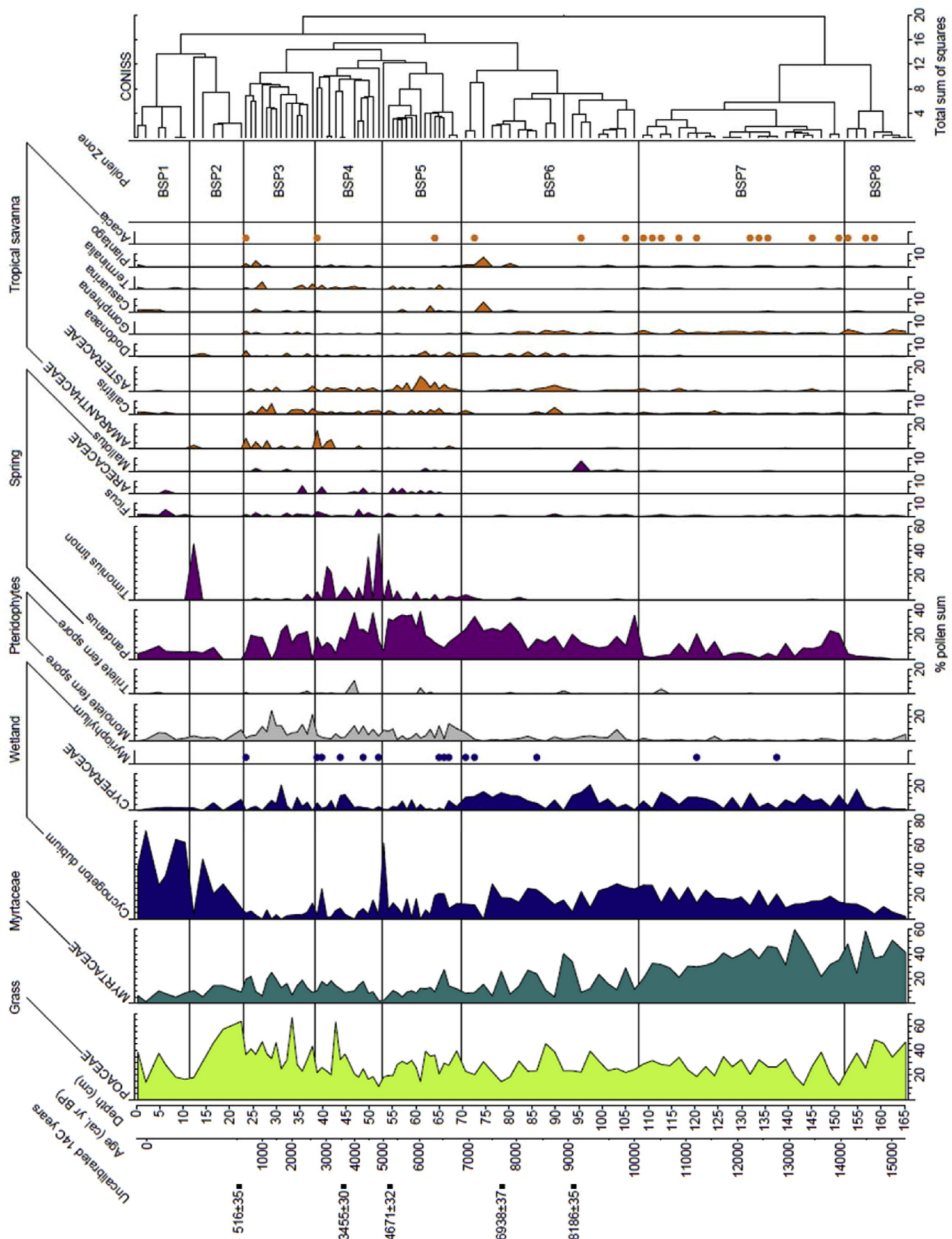


Fig. 5. Pollen percentage diagram of the Black Springs core (pteridophytes, Myrtaceous, grass, tropical savanna and wetland taxa included within the total pollen sum (dot = $\leq 1.5\%$)). Also shown are the results of cluster analysis which aided the identification of the eight pollen zones shown (labelled BSP1 – BSP8).

Table 2

Some information on pollen taxa encountered in the surface and core samples.

Pollen taxon name/family	Vegetation/taxonomic unit	Habitat/Environment
Ericaceae ^b	Exotic	Heathland
Podocarpus ^b	Exotic	Evergreen trees
Poaceae ^{a,b}	Grass	Grasses. Includes open dryland grasses and aquatic perennial grasses particularly <i>Phragmites karka</i>
Myrtaceae ^{a,b}	Myrtaceae	Shrubs and trees. Includes both dryland genera <i>Eucalyptus</i> and <i>Corymbia</i> and wetland genus <i>Melaleuca</i>
<i>Monolete fern spores</i> ^{a,b}	Pteridophytes	Ground ferns in moist locations
<i>Trilete fern spores</i> ^{a,b}	Pteridophytes	Ground ferns in moist locations
<i>Amyema Lorantheae</i> ^b	Spring	Mistletoe – epiphytic parasite
Areaceae ^{a,b}	Spring	Palms
<i>Breynia cernua</i> Euphorbiaceae ^b	Spring	Shrub common in monsoon forest and vine thicket, favours disturbance
<i>Elaeocarpus</i> Elaeocarpaceae ^{a,b}	Spring	Tropical evergreen trees and shrubs
<i>Euphorbia</i> Euphorbiaceae ^{a,b}	Spring	Rainforest herbs and shrubs
Euphorbiaceae ^b	Spring	Rainforest trees, herbs and shrubs
<i>Ficus</i> Moraceae ^{a,b}	Spring	Trees and vines common to monsoon forest and rainforest
<i>Mallotus</i> Euphorbiaceae ^{a,b}	Spring	Trees common to monsoon forest and rainforest, favours disturbance
<i>Pandanus</i> Pandanaceae ^{a,b}	Spring	Pachycaulous trees of vine thickets and watercourses
<i>Plectranthus congestus</i> Lamiaceae ^{a,b}	Spring	Herb and shrub common to monsoon forests
Sapotaceae ^b	Spring	Trees common to monsoon forests and rainforests
<i>Timonius timon</i> Rubiaceae ^{a,b}	Spring	Small tree common to monsoon forests and rainforests, may indicate disturbance
<i>Acacia</i> Mimosaceae ^{a,b}	Tropical savanna	Dryland trees and shrubs common to open vegetation
Acanthaceae ^b	Tropical savanna	Dryland herbs and shrubs
Amaranthaceae ^{a,b}	Tropical savanna	Dryland herbs and shrubs
Asteraceae (Tubuliflorae) ^{a,b}	Tropical savanna	Dryland herbs and shrubs common in open vegetation
<i>Banksia dentata</i> Proteaceae ^a	Tropical savanna	Dryland tree common near wet areas and on sandy soils
Brassicaceae ^{a,b}	Tropical savanna	Dryland herbs
<i>Callitris</i> Cupressaceae ^{a,b}	Tropical savanna	Dryland trees
<i>Casuarina</i> Casuarinaceae ^{a,b}	Tropical savanna	Dryland trees
<i>Codonocarpus cotinifolius</i>	Tropical savanna	Dryland shrub or tree. Common on sandy/loamy soils.
Gyrostemonaceae ^{a,b}		
<i>Dodonaea</i> Sapindaceae ^{a,b}	Tropical savanna	Trees or shrubs common in open woodlands
<i>Eremophila</i> Myoporaceae ^a	Tropical savanna	Shrubs and trees, commonly in arid areas
<i>Gomphrena</i> Amaranthaceae ^{a,b}	Tropical savanna	Dryland herbs, common on poor soils
<i>Newcastelia cladotricha</i> Verbenaceae ^{a,b}	Tropical savanna	Dryland herb
<i>Plantago</i> Plantaginaceae ^{a,b}	Tropical savanna	Dryland annual herbs
<i>Polygonum</i> Polygonaceae ^a	Tropical savanna	Dryland annual herbs
Proteaceae ^b	Tropical savanna	Dryland trees and shrubs
Sapindaceae ^b	Tropical savanna	Dryland trees and shrubs
<i>Terminalia</i> Combretaceae ^{a,b}	Tropical savanna	Dryland trees
<i>Tribulus</i> Zygophyllaceae ^{a,b}	Tropical savanna	Arid, dryland herbs
Verbenaceae ^{a,b}	Tropical savanna	Tropical trees, shrubs and herbs
<i>Colocasia esculenta</i> Araceae ^b	Wetland	Rhizomatous perennial herb – partially submerged
<i>Cyanogeton dubium</i> Juncaginaceae ^{a,b}	Wetland	Emergent perennial aquatic herb
Cyperaceae ^{a,b}	Wetland	Sedges – predominantly aquatic
Malvaceae ^b	Wetland	Annual herbs common to creeks and river edges
<i>Myriophyllum</i> Haloragaceae ^{a,b}	Wetland	Submerged aquatic herbs
<i>Typha</i> Typhaceae ^{a,b}	Wetland	Reeds/aquatic herbs

^a Identified in surface sample.^b Identified in down-core sample.

and springs in particular (Scott, 1992), and is often indicative of desiccation, summer drought, oxidation and warmer climates with seasonal drying (Carrión and Navarro, 2002), thus peak values in sample D4-2 are to be expected.

4.3. Fossil pollen and microcharcoal

The fossil pollen and charcoal record for Black Springs is presented in Fig. 5. CONISS aided the identification of eight distinct zones in the fossil pollen record based on cluster analysis, labelled BSP1 to BSP8 (Fig. 5). These zones are indicated on the summary diagram (Fig. 7). Table 2 lists the 42 taxa encountered in the fossil pollen dataset and their ecological affinities. Where values are discussed below they are averaged for the entire zone unless otherwise specified.

4.3.1. BSP8 (166–152 cm; inferred age ~15,000–14,000 cal yr BP)

Zone BSP8 is dominated by Poaceae (38%) and Myrtaceous taxa (43%), with very low values for spring vegetation (2%) and

pteridophytes. Some tropical savanna taxa are present in this zone, including *Acacia* and *Gomphrena*. Whilst the perennial aquatic *Cyanogeton dubium* is present (8%) other wetland taxa such as Cyperaceae are not well represented until the upper part of the zone where values rapidly increase from ~3% to 17%. Zone BSP8 has low charcoal and pollen accumulation rates, and the algal cyst *Pseudoschizaea* is absent.

4.3.2. BSP7 (152–108 cm; inferred age ~14,000–~10,000 cal yr BP)

The base of this zone is defined by an abrupt increase in spring and wetland taxa, in particular *Pandanus* and Cyperaceae. Spring taxa account for 8% of this zone whilst wetland taxa increase by 12% to comprise a quarter of the pollen sum. Values for Myrtaceae are high, however Poaceae abundances decrease to 26% and fluctuate more than within the previous zone. *Acacia* is more prolific in this period than within any of the other zones, with *Terminalia* also present in several samples. There is a peak in charcoal accumulation rates from 126 to 122 cm (~11,730–~11,380 cal yr BP). *Pseudoschizaea* is occasionally present.

4.3.3. BSP6 (108–70 cm; inferred age ~10,000–6840 cal yr BP)

In zone BSP6 a sustained increase in mound spring taxa occurs representing 26% of the total pollen sum in this zone. In particular *Pandanus* comprises 19% of the total pollen sum. Wetland taxa are abundant (>25%), in particular *C. dubium* and Cyperaceae, whilst Myrtaceae declined to 17%. Similarly tropical savanna taxa such as *Acacia* and *Terminalia* are less common in this zone. *Mallotus*, present sporadically throughout the core, has a distinct peak in this zone at 95.5 cm (~9150 cal yr BP), and similarly the dryland herb *Plantago* has a small peak at 74.5 cm (7320 cal yr BP). Accumulation rates for pollen and charcoal are low albeit with small increases in charcoal accumulation at 93.5 cm (9070 cal yr BP) and between 82 and 74 cm (8020–7310 cal yr BP). *Pseudoschizaea* is present sporadically in low values.

4.3.4. BSP5 (70–53 cm; inferred age 6840–4940 cal yr BP)

Tropical savanna taxa such as *Terminalia* and Asteraceae (Tubuliflorae) are a feature of zone BSP5 with the latter reaching highest values for the record (4% of the pollen sum). Pteridophytes also increase in abundance, with monolete fern spores also increasing in representation from 3% in zone BSP6 to 7% in zone BSP5. Wetland taxa are less common, Cyperaceae in particular experienced large declines, although there is a greater representation of spring taxa. In this zone, *C. dubium* appears to have an inverse relationship with *Pandanus*, most noticeable at 66 cm and 53 cm where declines in *Pandanus* are mirrored by increases in *C. dubium*. Myrtaceae values decline to ~11% whereas pollen from the vine thicket tree *T. timon* is more consistently present having been rare in preceding zones. *Pseudoschizaea* remains rare and charcoal and pollen accumulation rates remain low.

4.3.5. BSP4 (53–38 cm; inferred age 4940–2620 cal yr BP)

The base of zone BSP4 is marked by dramatic increases in *T. timon* and *Pseudoschizaea* accumulation rates. Two distinct peaks in *T. timon* book-end the zone (52–50 cm: 35–54%; 42–41 cm: 27–22%) and *Pseudoschizaea* accumulation rates increased rapidly from 50 cm reaching peak values at 39 cm (2680 cal yr BP). Charcoal and pollen accumulation rates remain low. The herb or small shrub *Amaranthaceae* increases in abundance at the top of the zone. Values of Poaceae, pteridophytes (primarily monolete fern spores) and Myrtaceae remain similar to zone BSP5, however *Terminalia* and the aquatic taxa *Myriophyllum* are more common.

4.3.6. BSP3 (38–23 cm; inferred age 2620–550 cal yr BP)

Poaceae increases slightly throughout to 38%, whilst wetland taxa and *T. timon* experience sharp declines with the latter virtually absent. *C. dubium* in particular reaches the lowest values of the entire record and *Myriophyllum* also becomes less common. *Pseudoschizaea* accumulation rates decline abruptly following a peak at 37 cm (2420 cal yr BP). Pteridophytes and Myrtaceae remain at similar levels to zone BSP4, however several tropical savanna tree and herb taxa are present including *Amaranthaceae*, *Callitris*, Asteraceae, *Dodonaea* and *Terminalia*. Pollen accumulation rates remain low whilst there is a small increase in charcoal accumulation towards the top of the zone.

4.3.7. BSP2 (23–11.5 cm; inferred age 550 cal yr BP – 230 cal yr BP)

Very high charcoal accumulation rates are characteristic of zone BSP2 whilst pollen accumulation is low. Poaceae is abundant at the base (>63%), although decreases up through (to 18%) concurrent with a dramatic increase in *C. dubium*. Myrtaceous taxa continue to fluctuate at levels similar to the previous three zones, whilst mound spring and tropical savanna taxa become less abundant. *Pandanus* is absent between 22.5 and 16.5 cm (530–360 cal yr BP) during the grass-dominated conditions at the base of this zone. An

anomalous sample with abundant *T. timon* (comprising 46% of the total pollen sum) is present at 12.5 cm immediately following a peak in charcoal accumulation. *Pseudoschizaea* is virtually absent.

4.3.8. BSP1 (11.5–0 cm; inferred age 230 cal yr BP – modern)

The uppermost pollen zone is dominated by wetland taxa. *C. dubium* reaches peak values for the entire record (>71% of the total pollen sum at 5 cm). Poaceae values are lower than in zone BSP2, while Myrtaceae also recorded the lowest values in the core (6%). *T. timon* and *Pseudoschizaea* are absent, although other mound spring taxa such as *Pandanus* are present albeit at lower values (7%). The majority of tropical savanna taxa present throughout the record are also less common with the exception of *Terminalia*. Charcoal accumulation rates decline, however pollen accumulation rates increase reaching peak values at 5 cm depth.

4.3.9. Comparison of the fossil pollen and surface sample datasets

The PCA biplot shown in Fig. 6 illustrates the relationship between the assemblages of the modern surface samples and those in the fossil dataset, zoned to aid interpretation. Samples MP3–5 and MP2–4 appear to contain assemblages significantly different to any found in the fossil record. This is likely a result of the surface

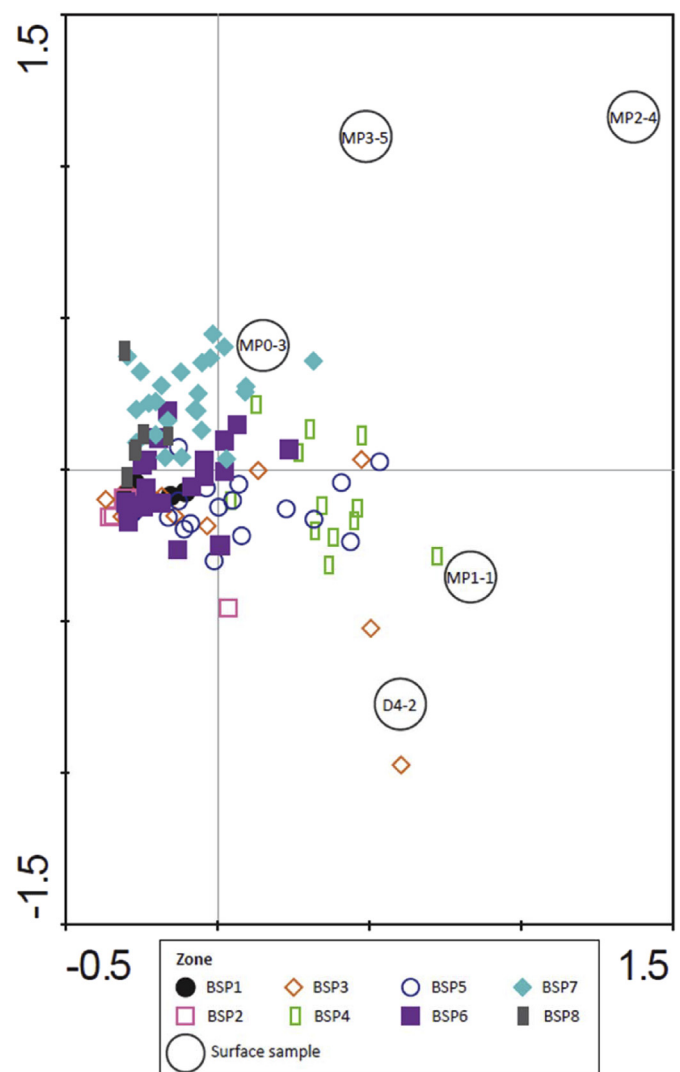


Fig. 6. PCA biplot of the Black Springs fossil and modern pollen data.

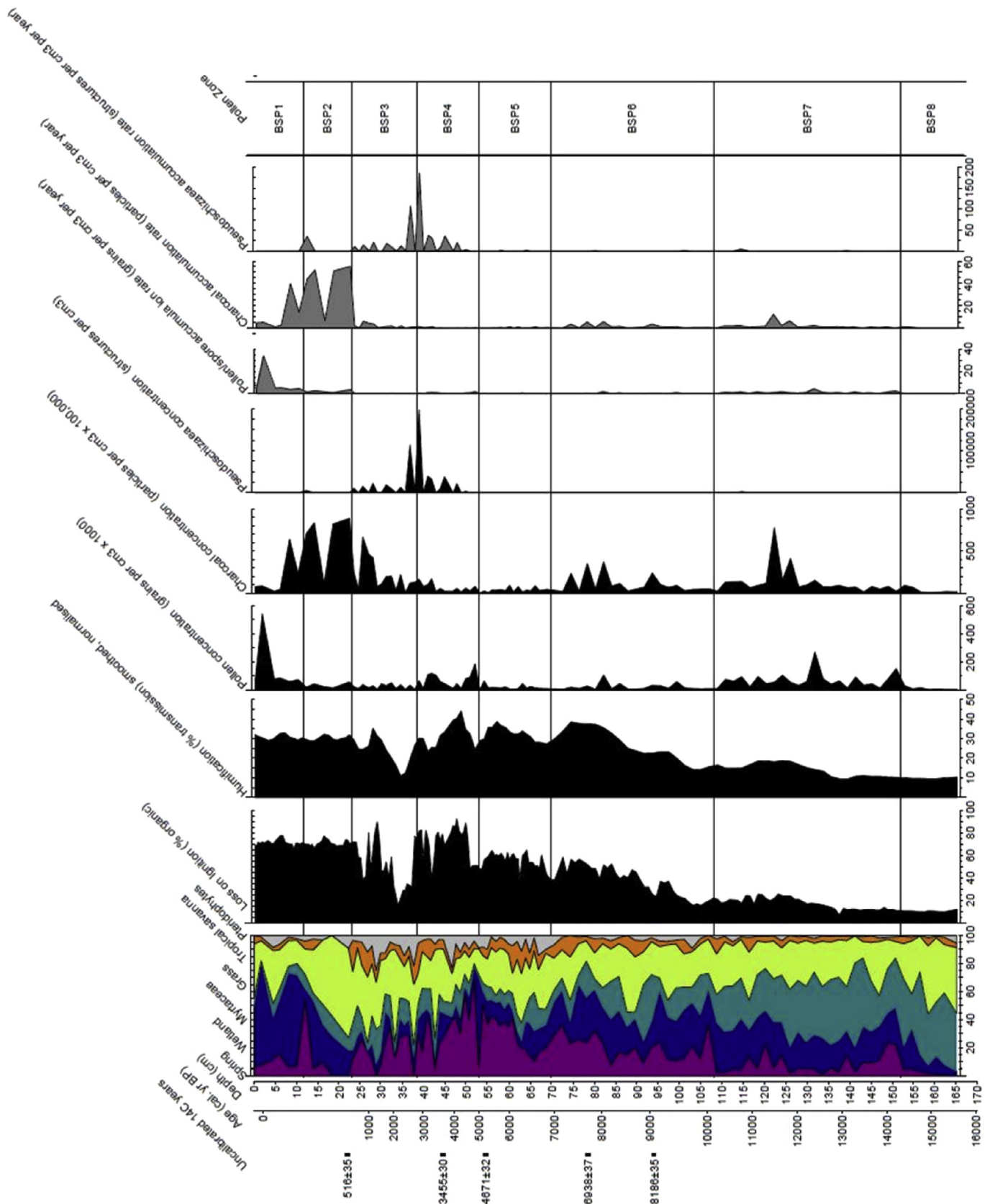


Fig. 7. Overview pollen diagram for Black Springs, with LOI and humification results and pollen zones BSP1 – BSP8 indicated. Pollen, charcoal and *Pseudoschizaea* accumulation rates and concentrations are also plotted.

samples reflecting their immediate vegetation. For instance, grass and tropical savanna taxa dominate sample MP3-5 which was collected from the surrounding savanna, whilst wetland taxa (sedges in particular) dominate sample MP2-4 which was collected from the mound spring wetland. Since the core was taken from the centre of the mound spring, it would appear that during the time period spanned by the fossil record a spring has always been present, and the peat mound has been of a sufficient size to mask the pollen signal from the surrounding savanna and wetland. The pollen assemblages from the surface samples taken from the peat mound itself (MP0-3, MP1-1 and D4-2) resemble those of the fossil record more closely.

The pollen assemblage of surface sample MP0-3, taken from the partially water inundated lower slopes of the mound, contains a pollen assemblage similar to zone BSP7 (~14,000–10,000 cal yr BP) suggesting two possibilities: that the environmental conditions during zone BSP7 were similar to the wet conditions currently seen at MP0-3; and/or that the mound may have been smaller than present bringing the inundated lower slopes closer to the coring site currently located at the top of the mound, making this zone similar floristically to MP0-3. Sample MP1-1, collected at the top of the mound where vegetation is dense and the peat saturated, is moderately similar to the assemblages of zone BSP4 (4940–2600 cal yr BP) and to some samples from zone BSP5 (6840–4940 cal yr BP). Since MP1-1 is taken from the same location as the core, it can be inferred that the mound was at or near its current extent during the mid Holocene and therefore conditions at the mound spring during the timespan covered by zone BSP4, and perhaps zone BSP5, were similar to the highly productive, saturated conditions currently seen at MP1-1. Surface sample D4-2, collected on the drier shoulder of the mound in the established monsoon vine thicket bears some resemblance to a small number of samples from zone BSP3 (2620–550 cal yr BP). This provides an indication that zone BSP3 contains great variability and that part of the

timespan covered by zone BSP3 featured conditions similar to those currently experienced on the spring shoulder.

4.4. Sediment analysis

LOI values are presented in Fig. 7 and exhibit an overall trend of increasing organic content up-core predominantly driven by growth of the peat mound gradually excluding alluvial sediments. Organic content is low from the base of the core to 137 cm (~13,000 cal yr BP) above which it increases, in particular above 102 cm (~9600 cal yr BP). Peak organic content occurs at 47.5 cm (4090 cal yr BP). Despite a number of fluctuations (in particular at 42 cm or 3340 cal yr BP) the core organic content remains high until 38 cm (2690 cal yr BP). Following this there is an abrupt decline in organics persisting until 25 cm (740 cal yr BP) then a short return to higher values between 33 cm and 27 cm (2036–1020 cal yr BP). The core organic content then increases and remains stable in the uppermost 24 cm of the core. Fig. 7 indicates that the changing LOI patterns tend to match the boundaries of the eight pollen zones. In summary zone BSP8 features low LOI values, which increase slightly throughout zones BSP7, BSP 6 and BSP5, particularly from 102 cm (~9600 cal yr BP). Zones BSP4 and BSP3 are distinguished by high and low LOI values respectively, whereas the uppermost zones BSP2 and BSP1 feature high, stable LOI values.

4.5. Humification

The Black Springs humification record is presented in both the summary diagram in Fig. 7 and in Fig. 8, with higher (lower) values of % transmission interpreted as indicating decreased (increased) humification of the peats and wetter (drier) conditions (Sillasoo et al., 2007). However, it should be noted prior to interpretation that low % transmission values from the base of the record to 102 cm (~9600 cal yr BP) are a result of the greater mineral content

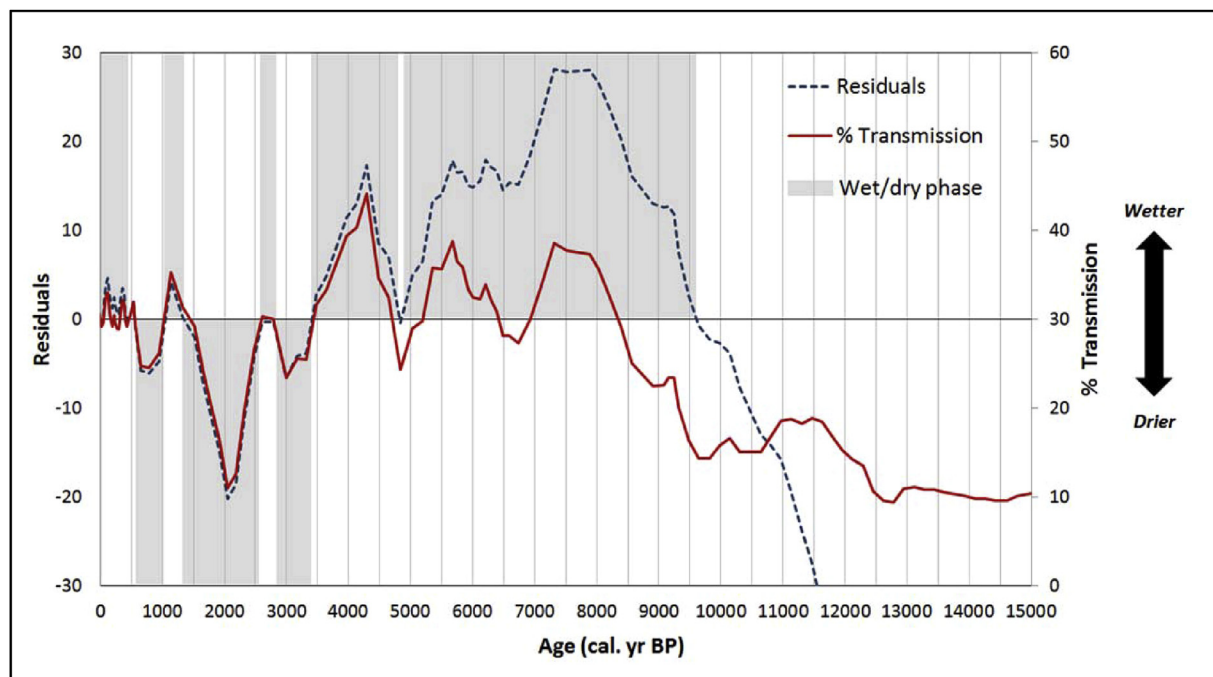


Fig. 8. Black Springs humification record plotted against age. The solid (red) line shows % transmission data smoothed (with a 3-point moving average) and normalised to LOI. The dashed (blue) line shows the detrended and smoothed residuals. Inferred wet and dry phases are indicated by grey shaded areas. Note - only oscillations from ~9600 cal yr BP to present are inferred as representing changes in bog surface wetness (see main text for further details). (For interpretation of the references to colour in this figure legend, the reader is referred to the web version of this article.)

Table 3

Summarised wet and dry shifts observed in the humification record (approximate depths and ages). The wettest and driest period is indicated by bold, italicised text.

Climate periods	From (depth - cm)	To (depth - cm)	From (age - cal. yr BP)	To (age - cal. yr BP)
Wet	4	23	Present	600
Dry	23	27	600	1000
Wet	27	29	1000	1300
Dry	29	39	1300	2600
Wet	39	40	2600	2800
Dry	40	43	2800	3400
Wet	43	51	3400	4700
Wet	53	103	4900	9600

of the peats. This is possibly due to both the peat mound being smaller than at present facilitating in-wash of catchment sediments and/or windblown sediment due to drier conditions. However, oscillations from 102 cm (~9600 cal yr BP) to present are inferred as representing changes primarily in bog surface wetness at Black Springs.

There are large oscillations in the humification record. Wet (dry) shifts have been defined where residuals clearly cross into positive (negative) values and are shown shaded in grey on Fig. 8, and are summarised in Table 3. Five wet and three dry shifts are defined. Residuals indicate peak moisture between 8500 and 7000 cal yr BP and peak aridity from 2600 to 1300 cal yr BP. The trend followed by the humification record is similar to the LOI data, and as such, is well correlated with the boundaries of the eight pollen zones.

5. Discussion

5.1. Mound spring morphology and environmental change at Black Springs

5.1.1. An increase in monsoon activity from ~14,000 cal yr BP

During the LGIT Black Springs appears to have been a juvenile spring, with an almost complete absence of spring pollen taxa prior to ~14,000 cal yr BP. These conditions continued until ~13,000 cal yr BP with higher minerogenic content of the sediments due to lower organic production at the spring and a greater likelihood of alluvial sediments being incorporated. The presence of the perennial aquatic *C. dubium* and Cyperaceae at this time also indicates a juvenile spring with a spring wetland.

Increasing organic content from ~13,000 cal yr BP reveals that the peat mound began to grow slowly during the transition from the late Pleistocene to early Holocene, with increases in the abundance of wetland taxa and sedges after this time indicating a more sustained spring wetland and outflow. Increased organic growth would have required more abundant vegetation at the spring with its subsequent decomposition contributing organic material to the site. Increases in spring taxa from ~14,000 cal yr BP indicate that this was the case. Denser vegetation at the spring, in context, is likely to have required an increase in spring discharge and, since outflow is related to meteoric recharge (McCarthy et al., 2010), it can be inferred that precipitation in this region of the Kimberley increased from ~14,000 cal yr BP. Comparisons with modern pollen assemblages indicate the presence of a small peat mound and wet conditions similar to those currently characteristic of the spring's lower slopes from ~14,000 cal yr BP.

Evidence for enhanced monsoon activity in the late Pleistocene is found preserved in other records across tropical Australasia. In the Kimberley these include higher-than-present lacustrine deposits at Lake Gregory at ~14,000 yr BP (Wyrwoll and Miller, 2001), speleothems from Ball Gown Cave showing increased monsoon rainfall from 13,000 cal yr BP (Denniston et al., 2013a), greater alluvial deposition along Cabbage Tree Creek in the Kimberley's north

from 12,000 yr BP (Wende et al., 1997), and an increase in moisture-indicative plant macrofossils from 11,500 yr BP (McConnell and O'Connor, 1997). This late Pleistocene shift in monsoon activity is also identified in marine records adjacent to the Kimberley, with elevated deposition of sediments derived from terrestrial runoff suggesting intensification of monsoon activity from 13,000 cal yr BP (Kuhnt et al., 2015). Offshore pollen records from this time also suggest increases in monsoon rainfall from 14,100 cal yr BP at the southern extent of the monsoonal zone (Van der Kaars and De Deckker, 2002; Van der Kaars et al., 2006) and from ~16,000 to 12,000 yr BP from the monsoon affected Timor Sea records (Van der Kaars, 1991; Kawamura et al., 2006; Kershaw et al., 2006).

5.1.2. An early Holocene precipitation maximum

In the early Holocene the peat mound appeared to grow rapidly in size with a dramatic increase in organic content from ~9600 cal yr BP indicating dense vegetation cover at the spring and the gradual exclusion of sediments deposited by runoff from the surrounding land surface. This increase in vegetation cover is reflected by the increases in spring taxa observed in the fossil record. The rapid growth of the mound would have required a large increase in precipitation, with humification analysis also showing elevated spring surface wetness from ~9600 cal yr BP and a particularly wet period between 8500 and 7000 cal yr BP. Taxa suggestive of wetter conditions also increase from this time including *Pandanus* - a tree common to moist and humid environments such as vine thickets and along watercourses, and the rainforest genus *Mallotus* which is most abundant at ~9150 cal yr BP. Wetland taxa also now comprise a large portion of the total pollen sum, in particular the perennial aquatic *C. dubium* which suggests standing water at the site. Increases in charcoal accumulation rates at 9070 and 8020 cal yr BP are indicative of greater biomass burning, likely to be a result of higher fuel loads at, and surrounding the spring.

Speleothem records from the southwest and eastern Kimberley also indicate wetter monsoon conditions in the early Holocene (Denniston et al., 2013a, 2013b), with the Cave KNI-51 record in particular indicating greatest precipitation between ~9000 and 7000 cal yr BP (Denniston et al., 2013b), matching the Black Springs record presented here. Pollen, mangrove clays, woods and organic muds from the Kimberley's north suggest extensive mangrove forests were established by 9000 cal yr BP and were sustained until at least 6000 yr BP, facilitated by increasing sea level, warmer post-glacial temperatures and enhanced freshwater input from a more active monsoon (Jennings, 1975; Thom et al., 1975; Proske et al., 2014). Pollen from the region's north also reflects woodland expansion at this time, with the occurrence of taxa dependent on moist soils suggestive of increased moisture (Proske et al., 2014). Quantitative estimates from offshore pollen records also indicate a thermal maximum at 8000 cal yr BP and peak precipitation between 7000 and 6000 cal yr BP (Van der Kaars et al., 2006).

5.1.3. Active and stable monsoon conditions until 5000 cal yr BP

The similarities between the pollen assemblages from the mid-late Holocene zone BSP4 (and to some extent zone BSP5) and sample MP1-1 collected at the coring location, currently at the mound's highest point, indicate that Black Springs appears to have reached its modern extent at least by the mid Holocene. The pollen, LOI and humification data presented here all suggest continued monsoon activity throughout the mid Holocene until ~5000 cal yr BP, albeit with reduced precipitation when compared to the early Holocene. For instance, the humification data identifies a wet phase persisting until 4900 cal yr BP, although residuals are lower than in the preceding period indicating a slight reduction in surface wetness. The similarities between the fossil pollen assemblages at this time to the modern pollen assemblages of the productive and saturated conditions in the centre of the mound also indicate an active monsoon. There is a clear change in pollen assemblages at 6840 cal yr BP as a result of the decreasing abundance of wetland taxa (particularly Cyperaceae) and increases in *T. timon* and ferns. *T. timon* is presently found growing on the drier slopes of Black Springs suggesting that whilst moist conditions persisted throughout the mid Holocene, precipitation and spring outflow were lower. Increased representation of dryland taxa such as *Terminalia* and Asteraceae also suggest that vegetation surrounding the spring was indicative of a drier climate.

Pollen data from marine core FR10/95 at the southern extent of the monsoonal zone also indicates high rainfall values between 7000 and 6000 cal yr BP (Van der Kaars et al., 2006), whilst speleothem records from Cave KNI-51 in the East Kimberley suggest an active but slightly weaker monsoon between 7000 and 5500 cal yr BP (Denniston et al., 2013b).

5.1.4. Increased variability from 5000 cal yr BP

From 5000 cal yr BP to present all proxies indicate increased environmental and climatic variability at Black Springs. All point to a short-lived drying phase at ~5000 cal yr BP where there is a sharp decrease in humification data and organic content suggesting decreased productivity at the spring, and perhaps increased aeolian sedimentation due to reduced monsoon rainfall. There is a change in the pollen assemblages at this time with clear decreases in taxa indicative of wetter conditions such as *Pandanus* and Myrtaceae (likely to be *Melaleuca*) in favour of vine thicket taxa common on the mound's drier slopes such as *T. timon*. Pollen from the FR10/95 marine core also indicates short term aridity at 5000 cal yr BP (Van der Kaars and De Deckker et al., 2002; Van der Kaars et al., 2006), concurrent with a period of dune building and sand mobilisation in the Gregory Lakes basin (Fitzsimmons et al., 2012). The KNI-51 speleothem record in the Kimberley's east shows evidence of reduced monsoonal precipitation from 4200 cal yr BP (Denniston et al., 2013b), whilst a decline in mangrove diversity at ~4000 cal yr BP in the northeast is argued to be a result of aridity (Proske, 2016). The discrepancies in timing of this event between records may indicate some intra- and inter-site variability, but also are within uncertainty in age control between records.

Wetter conditions at Black Springs appear to return from ~4700 cal yr BP until ~3400 cal yr BP as suggested by humification data, organic content and the presence of the aquatic genus *Myriophyllum*. However, whilst the monsoon appears active at this time taxa indicative of a drier environment increase in abundance including *T. timon* and *Terminalia* suggesting that the monsoon is weaker than earlier in the Holocene section of the record. The increase in *Pseudoschizaea*, which is indicative of desiccation, drought, oxidation and warmer climates with seasonal drying (Carrion and Navarro, 2002), supports this interpretation of the record. It is likely that *Pseudoschizaea* has been absent or rare in the record up to this time due to the active monsoon conditions in the

early-mid Holocene. A return to drier conditions between 3400 and 2800 cal yr BP is also suggested by the humification data, organic content and peak in *T. timon*, prior to a shift to wetter conditions which persists until 2600 cal yr BP. Increased late Holocene climatic variability is also observed at Cape St Lambert in the Kimberley's north as discrete dune building events (Lees et al., 1992).

5.1.5. Pronounced late Holocene aridity

Humification analysis show that the driest phase in the record occurs between 2600 and 1300 cal yr BP. This is concurrent with a sharp decline in organic content suggestive of decreased productivity and increased aeolian sedimentation due to a much less active monsoon. The slower growth rate during the late Holocene may also reflect the drier, less productive conditions at the mound and potentially even the deflation of some sediment. There is a shift in vegetation assemblages at 2600 cal yr BP, with the declining representation of aquatics such as *C. dubium* and *Myriophyllum* indicative of reduced standing water at the spring. The abrupt decline of *T. timon* alongside the continued representation of tropical savanna taxa including Amaranthaceae, *Callitris*, Asteraceae, *Dodonaea* and *Terminalia* also suggest drier conditions, whilst the reduction in *Pseudoschizaea* accumulation may reflect the onset of conditions too dry to sustain a large presence of an algal cyst which is typically most abundant in damp soils (Scott, 1992). The pollen assemblages during this time are similar in part to the modern assemblage from the dry shoulder of the mound also suggesting that conditions during the late Holocene were drier and variable. The tolerance of *Pandanus* to drought (Elevitch, 2006) may account for its continued presence in this section of the record despite the inferred drier conditions.

Evidence of drier conditions during the late Holocene can be seen in other records across the Kimberley. For instance, the rapid development of cheniers in the Victoria Delta between 2000 and 1200 yr BP may be the result of reduced fluvial input to the shelf (Lees, 1992). A dust record for this Black Springs core also shows an increase in dust flux to the Kimberley's northwest from the Lake Eyre basin and eastern Simpson Desert indicating anticyclonic circulation and stronger south-easterly trade winds associated with a more northerly ITCZ (McGowan et al., 2012). Speleothem records from the Kimberley's east also show decreasing precipitation from 4200 cal yr BP with the driest phase occurring 1500–1200 cal yr BP (Denniston et al., 2013b).

5.1.6. Transition to modern conditions during the last millennium

A short wet phase is suggested by the humification data from 1300 to 1000 cal yr BP, with a subsequent change to drier conditions from 1000–550 cal yr BP. There is a change in pollen assemblages at 550 cal yr BP correlated with shifts seen in the humification record and organic contents to stable values which persist through to present. A sharp increase in grass pollen at 550 cal yr BP indicates that the surrounding tropical savanna became more open. The simultaneous increase in charcoal accumulation may be related to taphonomic processes since high charcoal accumulation rates have been observed to parallel major vegetation changes in the Australian tropics (e.g. Kershaw et al., 2002; Proske et al., 2014). A peak in *T. timon* concurrent with a subsequent decline in charcoal accumulation at 260 cal yr BP is likely to be a response to burning since *T. timon* is a ready coloniser of disturbed and open sites (Space et al., 2003). In the last ~230 years an increasing abundance of the perennial aquatic *C. dubium* together with the return of *Pandanus* to the record can be interpreted as showing a ready supply of water at the site due to active monsoon conditions.

Evidence for active monsoon conditions in the Kimberley over the last couple of centuries are also seen in the Cave KNI-51

speleothem record which shows an elevated number of extreme rainfall events in the last 200 years (Denniston et al., 2015). However, shifts to modern conditions occurring in the last ~550 years are seen elsewhere in the Kimberley such as the development of modern floodplain settings at Parry Lagoons Wetlands in the northeast from at least 600 cal yr BP (Proske, 2016). Other northern Australian pollen records indicate a transition to modern conditions during the last millennium (Rowe, 2015; Stevenson et al., 2015). The discrepancies between these records may indicate variability between sites, but may also be a result of dating uncertainties.

5.2. Drivers of change

We infer that the increase in monsoonal rainfall seen in the Black Springs record from ~14,000 cal yr BP is likely to be driven predominantly by post-glacial sea-level rise. The drowning of the Sunda and Sahul shelves following the Last Glacial Maximum (LGM) was an important driver of change in tropical hydroclimate, facilitating increased moisture advection fuelling monsoon activity across tropical Australasia during the late Pleistocene (DiNezio and Tierney, 2013). Micropalaeontological, geomorphological and coral evidence indicates that the sea level rise in the northwest Australian region was moderate from 19,400 cal yr BP (De Deckker and Yokoyama, 2009) before becoming increasingly rapid in response to Meltwater Pulse 1A at 14,700–14,100 yr BP (Hanebuth et al., 2000) ultimately expanding the IPWP and facilitating increases in monsoonal precipitation (De Deckker et al., 2002). Recent high resolution marine records adjacent to the Kimberley have also proposed that enhanced Southern Hemisphere greenhouse forcing as a result of post-glacial CO₂ rise would have accentuated the southward displacement of the ITCZ during the Younger Dryas, and would have contributed to late Pleistocene increases in precipitation across this region (Kuhnt et al., 2015).

Wetter and warmer conditions in general were experienced across tropical Australasia during the early Holocene (Reeves et al., 2013) with several speleothem records attributing this to the transgression of the Sahul and Sunda shelves (Partin et al., 2007; Griffiths et al., 2009; Denniston et al., 2013a, 2013b). In northwest Australia there is evidence that sea level rise became more rapid in the early Holocene in response to Meltwater Pulse 1B at 11,500 cal yr BP (Collins et al., 2011), after which sea level continued to rise until at least the mid Holocene at ~7000–6500 yr BP (Van Andel and Veevers, 1967; Collins et al., 2011; Solihuddin et al., 2015). It is therefore likely that the early Holocene strengthening in monsoon activity seen in our record is primarily driven by the marine transgression.

Drying trends and a contraction of the IPWP are observed in several records across the tropical Australasian region during the mid Holocene connoting a northward shift of the ITCZ (Reeves et al., 2013). Evidence for a northward shift of the ITCZ at this time comes from the Pacific (Koutavas et al., 2006), Indian (Fleitmann et al., 2003) and Atlantic Oceans (Haug et al., 2001). A northward shift of the ITCZ would have reduced monsoon activity across northwest Australia as seen in the Black Springs record between ~7000 and 5000 cal yr BP and in the KNI-51 speleothem record (Denniston et al., 2013b).

Increasing climatic variability and drying trends observed in records across tropical Australasia during the late Holocene (e.g. Donders et al., 2007; Reeves et al., 2013) has been linked to the increase in frequency and amplitude of El Niño from 5000 yr BP seen in several climate models and records (e.g. Moy et al., 2002; Gagan et al., 2004; Conroy et al., 2008). Despite the currently muted effect of El Niño on the monsoon in the Kimberley, Denniston et al. (2013b) suggest that a stronger relationship existed

between ENSO and northwest Australia since the late Holocene possibly due to changes in the mean state of the tropical Pacific. Similarly, McRobie et al. (2015) observed a teleconnection between the northwest and ENSO during the last 3000 years. We therefore suggest that the increased variability superimposed on a general drying trend from ~5000 cal yr BP at Black Springs, with a more arid phase from 2600 cal yr BP to 1300 cal yr BP, is a result of increases in the frequency and/or intensity of El Niño events. The decreased strength of El Niño from 1500 to 1000 cal yr BP seen in a number of records (Rein et al., 2004; Stott et al., 2004) may also have been responsible for the wet phase seen in the humification data between 1300 and 1000 cal yr BP as the La Niña phase became more dominant. The discrepancies in timing of the dry shift between the Kimberley's palaeoclimate records are likely to be due, at least in part, to differences in precipitation gradients across the Australian tropics which are still seen in the region today (e.g. Bureau of Meteorology (2016)).

Denniston et al. (2013b) suggest that the relationship between ENSO and the Kimberley weakened in the last millennium, which may have driven the transition to modern conditions seen at Black Springs in the last 550 years. Fluctuations seen in Australia's archaeological signature during the last ~500 years may be a response by hunter-gatherers to these climate shifts (Williams et al., 2010). The ameliorating climatic conditions may have promoted population expansion in the Kimberley, higher fuel loads and potentially an increase in fire stick farming (McGowan et al., 2012). This may have driven the more open vegetation and elevated charcoal accumulation rates seen at Black Springs from 550 cal yr BP, as well as in the region's northeast and across the wider Australian tropics.

6. Conclusions

This extended record from Black Springs provides the first high resolution reconstruction of environmental change in the Kimberley which encompasses the Holocene period and possibly continues beyond into the late Pleistocene. The Black Springs peat archive preserves clear evidence of dramatic changes in the strength of the northwest Australian summer monsoon during this timeframe, with key shifts corresponding with tropical Australasian climatic change during the late Quaternary discussed in the OZ-INTIMATE synthesis (Reeves et al., 2013). Results from Black Springs reveal that the Kimberley's northwest experienced an increase in monsoon activity sometime after ~14,000 cal yr BP persisting until 7000 cal yr BP likely driven by post-glacial sea level rise. The monsoon gradually weakened over the next 2000 years with a proposed northward shift of the ITCZ, before becoming more variable and possibly even failing during the late Holocene associated with enhanced El Niño phases. Modern monsoon activity appears to have been established in the last 600 years.

Acknowledgements

This research was supported by the Kimberley Foundation Australia with 2015 fieldwork and majority of the laboratory research completed whilst the first author was the recipient of an Australian Postgraduate Award and an Australian Institute of Nuclear Science and Engineering (AINSE) Post Graduate Research Award. We would like to extend a special thank you to the Koeyers family of Drysdale River Station for providing excellent local knowledge and hospitality during both field trips to the Kimberley in 2005 and 2015. We would like to thank Mark Burrows for his assistance with humification analysis, and Joshua Soderholm for his assistance with detrending humification data. Thanks also go to Anson Mackay for advice regarding multivariate statistics, Peter

Veth and Jane Balme for their expertise regarding human occupation in the Kimberley, and Andy Hammond and the late Grahame Walsh for collecting the Black Springs core. The authors would like to thank three anonymous reviewers for their constructive comments on the manuscript.

References

- APSA Members, 2007. The Australasian Pollen and Spore Atlas V1.0. Australian National University, Canberra. Available at: <http://apsa.anu.edu.au/>.
- Ashok, K., Behara, S.K., Rao, S.A., Weng, H., Yamagata, T., 2007. El Niño Modoki and its possible teleconnection. *J. Geophys. Res.* 112 (C11007), 1–27.
- Aubert, M., 2012. A review of rock art dating in the Kimberley, Western Australia. *J. Archaeol. Sci.* 39, 573–577.
- Backwell, L.R., McCarthy, T.S., Wadley, L., Henderson, Z., Steininger, C.M., deKlerk, B., Barré, M., Lamothe, M., Chase, B.M., Woodborne, S., Susino, G.J., Bamford, M.K., Sievers, C., Brink, J.S., Rossouw, L., Pollarolo, L., Trower, G., Scott, L., d'Errico, F., 2014. Multiproxy record of late Quaternary climate change and Middle Stone Age human occupation at Wonderkrater, South Africa. *Quat. Sci. Rev.* 99, 42–59.
- Balme, J., 2000. Excavations revealing 40,000 years of occupation at Mimbi caves, south central Kimberley, Western Australia. *Aust. Archaeol.* 5 (1), 1–5.
- Barber, K., Charman, D., 2005. Holocene palaeoclimate records from peatlands. In: Mackay, A., Battarbee, R., Birks, J., Oldfield, F. (Eds.), *Global Change in the Holocene*. Hodder Education, Great Britain, pp. 210–222.
- Blaauw, M., Christen, J.A., 2011. Flexible paleoclimate age-depth models using an autoregressive gamma process. *Bayesian Anal.* 6, 457–474.
- Blackford, J.J., Chambers, F.M., 1993. Determining the degree of peat decomposition in peat-based palaeoclimatic studies. *Int. Peat J.* 5, 7–24.
- Boyd, W.E., 1990a. Mound springs. In: Tyler, M.J., Twidale, C.R., Davies, M., Wells, C.B. (Eds.), *Natural History of the North East Deserts*, vol. 6. Royal Society of South Australia Inc, pp. 107–118.
- Boyd, W.E., 1990b. Quaternary pollen analysis in the arid zone of Australia: dalhousie Springs, Central Australia. *Rev. Palaeobot. Palynol.* 64 (1–4), 331–341.
- Boyd, B., Luly, J., 2005. Inland mound springs. In: Whinam, J., Hope, G. (Eds.), *The Peatlands of the Australasian Region*. (Mires - from Siberia to Tierra del Fuego). Biologisches Zentrum der Österreichischen Landesmuseen, pp. 397–434.
- Brodie, R.S., Kilgour, B., Jacobson, G., Lau, J.E., 1998. Hydrogeology Map of Australia. Commonwealth of Australia (Geoscience Australia).
- Bronk Ramsey, C., 2013. OxCal Program, V4.2.2. Radiocarbon Accelerator Unit. University of Oxford. Available at: http://c14.arch.ox.ac.uk/oxcalhelp/hlp_contents.html.
- Bureau of Meteorology, 2016. <http://www.bom.gov.au/>.
- Burrows, M.A., Fenner, J., Haberle, S.G., 2014. Humidification in northeast Australia: dating millennial and centennial scale climate variability in the late Holocene. *Holocene* 24 (12), 1707–1718.
- Carrión, J.S., Navarro, C., 2002. Cryptogam spores and other non-pollen microfossils as sources of palaeoecological information: case studies from Spain. *Ann. Bot. Fenn.* 39, 1–14.
- Chambers, F.M., Beilman, D.W., Yu, Z., 2011. Methods for determining peat humification and for quantifying peat bulk density, organic matter and carbon content for palaeostudies of climate and peatland carbon dynamics. *Mires Peat* 7, 1–10.
- Chambers, F.M., Booth, R.K., De Vleeschouwer, F.D., Lamentowicz, M., Le Roux, G., Mauquoy, D., Nichols, J.E., van Geel, B., 2012. Development and refinement of proxy-climate indicators from peats. *Quat. Int.* 268, 21–33.
- Cobb, K.M., Westphal, N., Sayani, H.R., Watson, J.T., Di Lorenzo, E., Cheng, H., Edwards, R.L., Charles, C.D., 2013. Highly variable El Niño-southern oscillation throughout the Holocene. *Science* 339 (6115), 67–70.
- Collins, L.B., Testa, V., Zhao, J., Qu, D., 2011. Holocene growth history and evolution of the Scott Reef carbonate platform and coral reef. *J. R. Soc. West. Aust.* 94 (2), 239–250.
- Conroy, J.L., Overpeck, J.T., Cole, J.E., Shanahan, T.M., Steinitz-Kannan, M., 2008. Holocene changes in eastern tropical Pacific climate inferred from a Galápagos lake sediment record. *Quat. Sci. Rev.* 27, 1166–1180.
- De Deckker, P., Yokoyama, Y., 2009. Micropalaeontological evidence for late Quaternary sea-level changes in Bonaparte gulf, Australia. *Glob. Planet. Change* 66, 85–92.
- De Deckker, P., Tapper, N.J., van der Kaars, S., 2002. The status of the indo-pacific warm pool and adjacent land at the last glacial maximum. *Glob. Planet. Change* 35, 25–35.
- Denniston, R.F., Wyrwoll, K.-H., Asmerom, Y., Polyak, V.J., Humphreys, W.F., Cugley, J., Woods, D., LaPointe, Z., Peota, J., Greaves, E., 2013a. North Atlantic forcing of millennial-scale Indo-Australian monsoon dynamics during the Last Glacial period. *Quat. Sci. Rev.* 72, 159–168.
- Denniston, R.F., Wyrwoll, K.-H., Polyak, V.J., Brown, J.R., Asmerom, Y., Wanamaker Jr., A.D., LaPointe, Z., Ellerbroek, R., Bathelmes, M., Cleary, D., Cugley, J., Woods, D., Humphreys, W.F., 2013b. A Stalagmite record of Holocene Indonesian-Australian summer monsoon variability from the Australian tropics. *Quat. Sci. Rev.* 78, 155–168.
- Denniston, R.F., Villarini, G., Gonzales, A.N., Wyrwoll, K.-H., Polyak, V.J., Ummenhofer, C.C., Lachniet, M.S., Wanamaker, A.D., Humphreys, W.F., Woods, D., Cugley, J., 2015. Extreme rainfall activity in the Australian tropics reflects changes in the El Niño/Southern Oscillation over the last two millennia. *Proc. Natl. Acad. Sci.* 112 (15), 4576–4581.
- Department of Environment and Conservation, 2012. *Understanding Wetlands. A Guide to Managing and Restoring Wetlands in Western Australia – Wetland Vegetation and Flora, Part 2: Kimberley*.
- DiNezio, P.N., Tierney, J.E., 2013. The effect of sea level on glacial Indo-Pacific climate. *Nat. Geosci.* 6, 485–491.
- Donders, T.H., Haberle, S.G., Hope, G., Wagner, F., Visscher, H., 2007. Pollen evidence for the transition of the eastern Australian climate system from the post-glacial to the present-day ENSO mode. *Quat. Sci. Rev.* 26, 1621–1637.
- Elevitch, C.R. (Ed.), 2006. *Traditional Trees of Pacific Island: Their Culture, Environment, and Use*. Permanent Agriculture Resources, Holualoa, Hawaii.
- Fifield, L.K., Bird, M.I., Turney, C.S.M., Hausladen, P.A., Santos, G.M., di Tada, M.L., 2001. Radiocarbon dating of the human occupation of Australia prior to 40ka BP – successes and pitfalls. *Radiocarbon* 43, 1139–1145.
- Fitzsimmons, K.E., Miller, G.H., Spooner, N.A., Magee, J.W., 2012. Aridity in the monsoon zone as indicated by desert dune formation in the Gregory Lakes basin, northwestern Australia. *Aust. J. Earth Sci.* 59 (4), 469–478.
- Fleitmann, D., Burns, S.J., Mudelsee, M., Neff, U., Kramers, J., Mangini, A., Matter, A., 2003. Holocene forcing of the Indian Monsoon recorded in a stalagmite from southern Oman. *Science* 300, 1737–1739.
- Gagan, M.K., Hendy, E.J., Haberle, S.G., Hantoro, W.S., 2004. Post-glacial evolution of the indo-pacific warm pool and El Niño-southern oscillation. *Quat. Int.* 118/119, 127–143.
- Gaiser, E., Ruhland, K.M., 2010. Diatoms as indicators of environmental change in wetlands and peatlands. In: Smol, J.P., Stoermer, E.F. (Eds.), *The Diatoms: Applications for the Environmental and Earth Sciences*. Cambridge University Press, Cambridge, pp. 473–496.
- Government of Western Australia, 2011. *Kimberley Science and Conservation Strategy*.
- Griffiths, M.L., Drysdale, R.N., Gagan, M.K., Zhao, J.-x., Ayliffe, L.K., Hellstrom, J.C., Hantoro, W.S., Frisia, S., Feng, Y.-x., Cartwright, I., Pierre, E. St. Fischer, M.J., Suwargadi, B.W., 2009. Increasing Australian-Indonesian monsoon rainfall linked to early Holocene sea-level rise. *Nat. Geosci.* 2, 636–639.
- Grimm, E.C., 1987. CONISS: a FORTRAN 77 program for stratigraphically constrained cluster analysis by the method of incremental sum of squares. *Comput. Geosci.* 13, 13–35.
- Grimm, E.C., 1991. *Tilia Program Ver. 2.0 B4*. Illinois Museum, Springfield.
- Grimm, E.C., 2004. *TGView Version 2.0.2*. Illinois State Museum, Springfield, IL, USA.
- Hall, V.A., 1989. A comparison of grass foliage, moss pollsters and soil surfaces as pollen traps in modern pollen rain studies. *Circaea* 6, 63–69.
- Hall, V.A., 1990. Some problems encountered in identifying Phragmites pollen in modern and fossil pollen assemblages. *Circaea* 8 (1), 17–19.
- Hanebuth, T., Stattegger, K., Grootes, P.M., 2000. Rapid flooding of the Sunda Shelf: a late-glacial sea level record. *Science* 288 (5468), 1033–1035.
- Haslam, S.M., 1972. Biological flora of the British isles Phragmites communis. *J. Ecol.* 60, 585–610.
- Haug, G.H., Hughen, K.A., Sigman, D.M., Peterson, L.C., Röhl, U., 2001. Southward migration of the intertropical convergence zone through the Holocene. *Science* 293 (5533), 1304–1308.
- Head, L., Fullager, R., 1992. Palaeoecology and archaeology in the east Kimberley. *Quat. Australasia* 10 (1), 27–31.
- Heiri, O., Lotter, A.F., Lemcke, G., 2001. Loss on ignition as a method for estimating organic and carbonate content in sediments: reproducibility and comparability of results. *J. Paleolimnol.* 25 (1), 101–110.
- Hiscock, P., O'Connor, S., Balme, J., Maloney, T., 2016. World's earliest ground-edge axe production coincides with human colonisation of Australia. *Aust. Archaeol.* 82 (1), 2–11.
- Hogg, A.G., Hua, Q., Blackwell, P.G., Niu, M., Buck, C.E., Guilderson, T.P., Heaton, T.J., Palmer, J.G., Reimer, P.J., Reimer, R.W., Turney, C.S.M., Zimmerman, S.R.H., 2013. SHCAL13 southern Hemisphere calibration, 0–50,000 years cal BP. *Radiocarbon* 55 (4), 1889–1903.
- Huang, B., Mehta, V.M., 2004. The response of the Indo-Pacific Warm Pool to interannual variations in net atmospheric freshwater. *J. Geophys. Res.* 109, C06022.
- Jennings, J.N., 1975. Desert dunes and estuarine fill in the Fitzroy estuary (North-Western Australia). *Catena* 2 (C), 215–262.
- Jourdain, N.C., Sen Gupta, A., Taschetto, A.S., Ummenhofer, C.C., Moise, A.F., Ashok, K., 2013. The Indo-Australian monsoon and its relationship to ENSO and IOD in reanalysis data and the CMIP3/CMIP5 simulations. *Clim. Dyn.* 41, 3073–3102.
- Kawamura, H., Holbourn, A., Kuhnt, W., 2006. Climate variability and land-ocean interactions in the Indo Pacific Warm Pool: a 460-ka palynological and organic geochemical record from the Timor Sea. *Mar. Micropaleontol.* 59 (1), 1–14.
- Keenan, T.D., Morton, B.R., Manton, M.J., Holland, G.J., 1989. The Island thunderstorm experiment (ITEX) – a study of tropical thunderstorms in the maritime continent. *Bull. Am. Meteorol. Soc.* 7, 152–159.
- Keenan, T.D., Rutledge, S.A., Carbone, R.E., Wilson, J.W., Takahashi, T., Moncrieff, M.W., Holland, G.J., Tapper, N.J., Platt, C.M.R., Hacker, J.M., Saito, K., Crook, J., 2000. The maritime continent thunderstorm experiment [MCTEX]: overview and some results. *Bull. Am. Meteorol. Soc.* 81 (10), 2433–2455.
- Kershaw, A.P., 1979. Local pollen deposition in aquatic sediments on the Atherton Tableland, north-eastern Australia. *Aust. J. Ecol.* 4, 253–263.
- Kershaw, A.P., Clark, J.S., Gill, A.M., 2002. A history of fire in Australia. In: Bradstock, R., Williams, J., Gill, A.M. (Eds.), *Flammable Australia: the Fire*

- Regimes and Biodiversity of a Continent. Cambridge University Press, Cambridge, pp. 3–25.
- Kershaw, P., van der Kaars, S., Moss, P., Opdyke, B., Guichard, F., Rule, S., Turney, C., 2006. Environmental change and the arrival of people in the Australian region. *Before Farming* 1 (2), 1–24.
- Koutavas, A., Lynch-Stieglitz, J., Marchittom Jr., T.M., Sachs, J.P., 2002. El Niño-like pattern in ice age tropical Pacific sea surface temperature. *Science* 297, 226–230.
- Koutavas, A., deMenocal, P.B., Olive, G.C., Lynch-Stieglitz, J., 2006. Mid-Holocene El Niño-Southern Oscillation (ENSO) attenuation revealed by individual foraminifera in eastern tropical Pacific sediments. *Geology* 34 (12), 993–996.
- Kuhnt, W., Holbourn, A., Xu, J., Opdyke, B., De Deckker, P., Röhl, U., Muldsee, M., 2015. Southern Hemisphere control on Australian monsoon variability during the late deglaciation and Holocene. *Nat. Commun.* 6 (5916), 1–7.
- Lees, B.G., 1992. The development of a chenier sequence on the Victoria Delta, Joseph Bonaparte gulf, northern Australia. *Mar. Geol.* 103 (1), 215–224.
- Lees, B.G., Yanchou, L., Price, D.M., 1992. Thermoluminescence dating of dunes at Cape St. Lambert, east Kimberleys, northwestern Australia. *Mar. Geol.* 106 (1), 131–139.
- Macphail, M.K., Pemberton, M., Jacobson, G., 1999. Peat mounds of southwest Tasmania: possible origins. *Aust. J. Earth Sci.* 46, 667–677.
- Marx, S.K., McGowan, H.A., Kamber, B.S., 2009. Long-range dust transport from eastern Australia: a proxy for Holocene aridity and ENSO induced climate variability. *Earth Planet. Sci. Lett.* 282, 167–177.
- McBride, J.L., 1987. The Australian summer monsoon. In: Chang, C.P., Krishnamurti, T.N. (Eds.), *Monsoon Meteorology*. Oxford University Press, New York, pp. 203–231.
- McBride, J.L., Nicholls, N., 1983. Seasonal relationships between Australian rainfall and the southern oscillation. *Mon. Weather Rev.* 111, 1998–2004.
- McCarthy, T.S., Ellery, W.N., Backwell, L., Marren, P., de Klerk, B., Tooth, S., Brandt, D., Woodborne, S., 2010. The character, origin and palaeoenvironmental significance of the Wonderkrater spring mound, South Africa. *J. Afr. Earth Sci.* 58, 115–126.
- McConnell, K., O'Connor, S., 1997. 40,000 Year record of food plants in the southern Kimberley ranges, Western Australia. *Aust. Archaeol.* 45, 20–31.
- McGowan, H., Marx, S., Moss, P., Hammond, A., 2012. Evidence of ENSO megadrought triggered collapse of prehistory Aboriginal society in northwest Australia. *Geophys. Res. Lett.* 39 (22), L22702.
- McGregor, H.V., Gagan, M.K., 2004. Western Pacific coral δ18O records of anomalous Holocene variability in the El Niño-southern oscillation. *Geophys. Res. Lett.* 31, L11204.
- McPhaden, M.J., 2004. Evolution of the 2002/03 El Niño*. *Bull. Am. Meteorol. Soc.* 85 (5), 677–695.
- McRobie, F.H., Stember, T., Wyrwoll, K.-H., 2015. Transient coupling relationships of the Holocene Australian monsoon. *Quat. Sci. Rev.* 121, 120–131.
- Meyers, G., McIntosh, P., Pigot, L., Pook, M., 2007. The years of El Niño, La Niña, and interactions with the tropical Indian Ocean. *J. Clim.* 20, 2872–2880.
- Mooney, S.D., Harrison, S.P., Bartlein, P.J., Daniau, A.-L., Stevenson, J., Brownlie, K.C., Buckman, S., Cupper, M., Luly, J., Black, M., Colhoun, E., D'Costa, D., Dodson, J., Haberle, S., Hope, G.S., Kershaw, P., Kenyon, C., McKenzie, M., Williams, N., 2011. Late Quaternary fire regimes of Australia. *Quat. Sci. Rev.* 30, 28–46.
- Mooney, S.D., Tinner, W., 2011. The analysis of charcoal in peat and organic sediments. *Mires Peat* 7 (9), 1–18.
- Moss, P.T., 2013. Palynology and its application to geomorphology. In: Shroder, J.F., Switzer, A.D., Kennedy, D.M. (Eds.), *Treatise on Geomorphology*. Academic Press, San Diego, CA, United States, pp. 315–325.
- Moss, P.T., Tibby, J., Petherick, L., McGowan, H., Barr, C., 2013. Late Quaternary vegetation history of north stradbroke Island, Queensland, Eastern Australia. *Quat. Sci. Rev.* 74, 257–272.
- Moy, C.M., Seltzer, G.O., Rodbell, D.T., Anderson, D.M., 2002. Variability of El Niño/southern oscillation activity at millennial timescales during the Holocene epoch. *Nature* 420 (6912), 162–165.
- Owen, R.B., Renaut, R.W., Hover, V.C., Ashley, G.M., Muasya, A.M., 2004. Swamps, springs and diatoms: wetlands of the semi-arid Bogoria-Baringo Rift, Kenya. *Hydrobiologia* 518, 59–78.
- Partin, J.W., Cobb, K.M., Adkins, J.F., Clark, B., Fernandez, D.P., 2007. Millennial-scale trends in west Pacific warm pool hydrology since the Last Glacial maximum. *Nature* 449 (7161), 452–455.
- Ponder, W.F., 1986. Mound springs of the great artesian basin. In: De Deckker, P., Williams, W.D. (Eds.), *Limnology in Australia*. CSIRO, Dordrecht, pp. 403–420.
- Power, S., Casey, T., Folland, C., Colman, A., Mehta, V., 1999. Inter-decadal modulation of the impact of ENSO on Australia. *Clim. Dyn.* 15, 319–324.
- Proske, U., 2016. Holocene freshwater wetland and mangrove dynamics in the eastern Kimberley, Australia. *J. Quat. Sci.* 31 (1), 1–11.
- Proske, U., Heslop, D., Haberle, S., 2014. A Holocene record of coastal landscape dynamics in the eastern Kimberley region, Australia. *J. Quat. Sci.* 29 (2), 163–174.
- Reeves, J.M., Bostock, H.C., Ayliffe, L.K., Barrows, T.T., De Deckker, P., Devriendt, L.S., Dunbar, G.B., Drysdale, R.N., Fitzsimmons, K.E., Gagan, M.K., Griffiths, M.L., Haberle, S.G., Jansen, J.D., Krause, C., Lewis, S., McGregor, H.V., Mooney, S.D., Moss, P., Nanson, G.C., Purcell, A., van der Kaars, S., 2013. Palaeoenvironmental change in tropical Australasia over the last 30,000 years - a synthesis by the OZ-INTIMATE group. *Quat. Sci. Rev.* 74, 97–114.
- Rein, B., Lückge, A., Sirocko, F., 2004. A major Holocene ENSO anomaly during the Medieval period. *Geophys. Res. Lett.* 31, L17211.
- Risbey, J.S., Pook, M.J., McIntosh, P.C., Wheeler, M.C., Hendon, H.H., 2009. On the remote drivers of rainfall variability in Australia. *Mon. Weather Rev.* 137 (10), 3233–3253.
- Rowe, C., 2015. Late Holocene swamp transition in the Torres Strait, northern tropical Australia. *Quat. Int.* 385, 56–68.
- Scott, L., 1982a. A Late Quaternary pollen records from the Transvaal bushveld, South Africa. *Quat. Res.* 17, 339–370.
- Scott, L., 1982b. A 5000-year old pollen record from spring deposits in the bushveld at the north of the Soutpansberg, South Africa. *Palaeoecol. Afr.* 14, 45–55.
- Scott, L., 1988. Holocene environmental change at western Orange Free State pans, South Africa, inferred from pollen analysis. *Palaeoecol. Afr.* 19, 109–118.
- Scott, L., 1992. Environmental implications and origin of microscopic *Pseudoschizaea Thiergart* and *Frantz Ex R. Potonie emend.* in sediments. *J. Biogeogr.* 19 (4), 349–354.
- Scott, L., Vogel, J.C., 1983. Late Quaternary pollen profile from the transvaal Highveld, South Africa. *South Afr. J. Sci.* 79, 266–272.
- Scott, L.N., Nyakale, M., 2002. Pollen indications of Holocene palaeoenvironments at Florisbad spring in the central free state, South Africa. *Holocene* 12 (4), 497–503.
- Scott, L., Holmgren, K., Siep Talma, A., Wooborne, S., Vogel, J.C., 2003. Age interpretation of the Wonderkrater spring sediments and vegetation change in the Savanna Biome, Limpopo province, South Africa. *South Afr. J. Sci.* 99, 484–488.
- Shulmeister, J., 1992. A Holocene pollen record from lowland tropical Australia. *Holocene* 2 (2), 107–116.
- Shulmeister, J., Lees, B.G., 1995. Pollen evidence from tropical Australia for the onset of an ENSO-dominated climate at c. 4000 BP. *Holocene* 5 (1), 10–18.
- Sillasoo, Ü., Mauquoy, D., Blundell, A., Charman, D., Blaauw, M., Daniell, J.R.G., Toms, P., Newberry, J., Chambers, F.M., Karofeld, E., 2007. Peat multi-proxy data from Männikjärve bog as indicators of late Holocene climate changes in Estonia. *Boreas* 36, 20–37.
- Solihuddin, T., Collins, L.B., Blakeway, D., O'Leary, M.J., 2015. Holocene coral reef growth and sea level in a macrotidal, high turbidity setting: cockatoo Island, Kimberley Bioregion, northwest Australia. *Mar. Geol.* 359, 50–60.
- Space, J.C., Waterhouse, B.M., Miles, J.E., Tiobech, J., Rengulbai, K., 2003. Report to the Republic of Palau on Invasive Plant Species of Environmental Concern. USDA Forest Service, Honolulu.
- Stevenson, J., Brockwell, S., Rowe, C., Proske, U., Shiner, J., 2015. The palaeoenvironmental history of Big Willum Swamp, Weipa: an environmental context for the archaeological record. *Aust. Archaeol.* 80, 17–31.
- Stott, L., Poulsen, C., Lund, S., Thunell, R., 2002. Super ENSO and global climate oscillations at millennial time scales. *Science* 297, 222–226.
- Stott, L., Cannariato, K., Thunell, R., Haug, G.H., Koutavas, A., Lund, S., 2004. Decline of surface temperature and salinity in the western tropical Pacific Ocean in the Holocene epoch. *Nature* 431, 56–59.
- Suppiak, R., 1992. The Australian summer monsoon: a review. *Prog. Phys. Geogr.* 16 (3), 283–318.
- Taschetto, A.S., Haarsma, R.J., Sen Gupta, A., Ummenhofer, C.C., Hill, K.J., England, M.H., 2010. Australian monsoon variability driven by a Gill–Matsuno-type response to central west Pacific warming. *J. Clim.* 23, 4717–4736.
- Ter Braak, C.J.F., Prentice, I.C., 1988. A theory of gradient analysis. *Adv. Ecol. Res.* 18, 271–317.
- Ter Braak, C.J.F., Šmilauer, P., 2002. *CANOCO for Windows* 4.5.
- Thom, B.G., Wright, L.D., Coleman, J.M., 1975. Mangrove ecology and deltaic-estuarine geomorphology: Cambridge gulf-ord river, western Australia. *J. Ecol.* 63 (1), 203–232.
- Van Andel, T.H., Veevers, J.J., 1967. Morphology and Sediments of the Timor Sea. Bureau of Mineral Resources, Geology and Geophysics. Canberra Bulletin 083.
- Van der Kaars, W.A., 1991. Palynology of eastern Indonesian marine piston-cores: a late Quaternary vegetational and climatic record for Australasia. *Palaeogeogr. Palaeoclimatol. Palaeoecol.* 85 (3), 239–302.
- Van der Kaars, S., De Deckker, P., 2002. A Late Quaternary pollen record from deep-sea core Fr10/95, GC17 offshore Cape Range Peninsula, northwestern Western Australia. *Rev. Palaeobot. Palynol.* 120 (1–2), 17–39.
- Van der Kaars, S., De Deckker, P., Ginge, F.X., 2006. A 100 000-year record of annual and seasonal rainfall and temperature for northwestern Australia based on a pollen record obtained offshore. *J. Quat. Sci.* 21 (8), 879–889.
- Van Zinderen Bakker, E.M., 1995. Archaeology and palynology. *South Afr. Archaeol. Bull.* 50 (162), 98–105.
- Wallis, L., 2001. Environmental history of northwest Australia based on phytolith analysis at Carpenter's Gap 1. *Quat. Int.* 83–85, 103–117.
- Webster, P.J., Palmer, T.N., 1997. The past and future of El Niño. *Nature* 390, 562–564.
- Wende, R., Nanson, G.C., Price, D.M., 1997. Aeolian and fluvial evidence for late Quaternary environmental change in the east Kimberley of western Australia. *Aust. J. Earth Sci.* 44 (4), 519–526.
- Wheeler, M.C., Hendon, H.H., Cleland, S., Meinke, H., Donald, A., 2009. Impacts of the Madden-Julian oscillation on Australian rainfall and circulation. *J. Clim.* 22 (6), 1482–1498.
- Williams, A.N., Ulm, S., Goodwin, I.D., Smith, M., 2010. Hunter-gatherer response to late Holocene climatic variability in northern and central Australia. *J. Quat. Sci.* 25 (6), 831–838.
- Wyrwoll, K.H., Miller, G.H., 2001. Initiation of the Australian summer monsoon 14,000 years ago. *Quat. Int.* 83 (5), 119–128.